POLITECNICO DI TORINO

Corso di Laurea Magistrale
in Ingegneria per l'Ambiente ed il Territorio

Tesi di Laurea Magistrale

Modelling the dispersion of plant protection products in the subsoil

Relatore
Prof. ssa Tiziana Tosco

Candidata
Aurora Audino

Anno Accademico 2018/2019

“All models are wrong, but some are useful.”

George Box

Table of contents

1. Introduction

The world and its population are facing many challenges nowadays.

Achieving sustainable production and ensuring food security while preserving the life on land and the environment from pollution are some of the goals of the 2030 Agenda for Sustainable Development, adopted by all United Nations Member States in 2015 (United Nations, 2015). The world population is 7.7 billion now and it will reach 8.5 billion in 2030 (10% increase) and 9.7 billion in 2050 (26% increase) (United Nations, 2019).

This means that an increasing demand for food has to coexist with an increasing attention to the human and environmental health. Due to the population growth and the limited availability of additional agricultural land, there will to a large extent be the necessity of rising the productivity of the land already being farmed today. Reducing yield losses is a major challenge that could be achieved, among other technical solutions, also by an efficient use of plant protection products, and in particular pesticides, in order to raise the agricultural output (Popp, et al., 2013).

On the other hand conventional pesticides are considered harmful because of their toxicity and their environmental impact. Some pesticides have been banned from use, some have very high toxicity levels, some others have been identified as carcinogenic or have potentials as carcinogens (Osman & Abdulrahman, 2003). Two of the pesticide's main drawbacks are related to their residuals and their non-target effects on humans health and on the environment. It is estimated that 90% of applied pesticides are lost during or after application. As a matter of fact, pesticides can spread to near non-target surfaces. Also, pesticides can infiltrate in the soil and run off into waterways or leach into groundwater. Moreover weather conditions influence the transport of pesticides during and after application. The effect of the wind or precipitation for example can increase the mobility of pesticides, contributing in the dispersion of the agrochemicals in the subsoil or near water bodies (e.g. rivers, aquifers).

Nano-pesticides have been identified as an emerging solution to traditionally used pesticides and represent an attractive field of research (Worrall, et al., 2018). Nano-pesticides, that are conventional pesticides coupled with nano-particles, have diverse advantages. They can increase the apparent solubility of poorly soluble active ingredients, lower and target the release of the

active ingredient and protect the active ingredient against early degradation (Kah & Hofmann, 2014). These properties overcome the problem of uncontrolled diffusion and consequently uncontrolled soil, water and air contamination and allow to avoid the use of surplus active ingredient usually applied for the conventional pesticides.

This thesis is part of the research project "NANOGRASS - Development of a NANO-herbicide formulation to minimize the impact of aGRochemicAls on Soil and Subsoil". This is a two year project, carried out by the Groundwater Engineering group of 'Politecnico di Torino', with the aim of reducing the uncontrolled dispersion of agrochemicals in the environment (Tosco, 2017). The project focus is on the study of new herbicide formulations with a lower environmental impact. A conceptual representation of the aim of the project is represented in Figure 1. The representation shows that the new nano-herbicide formulation enhances the target effect and reduces the potential risks of soil, water and air contamination, compared to a traditional one. Due to its more controlled release, the formulation also handles the problems of agrochemicals over dose and losses during application.

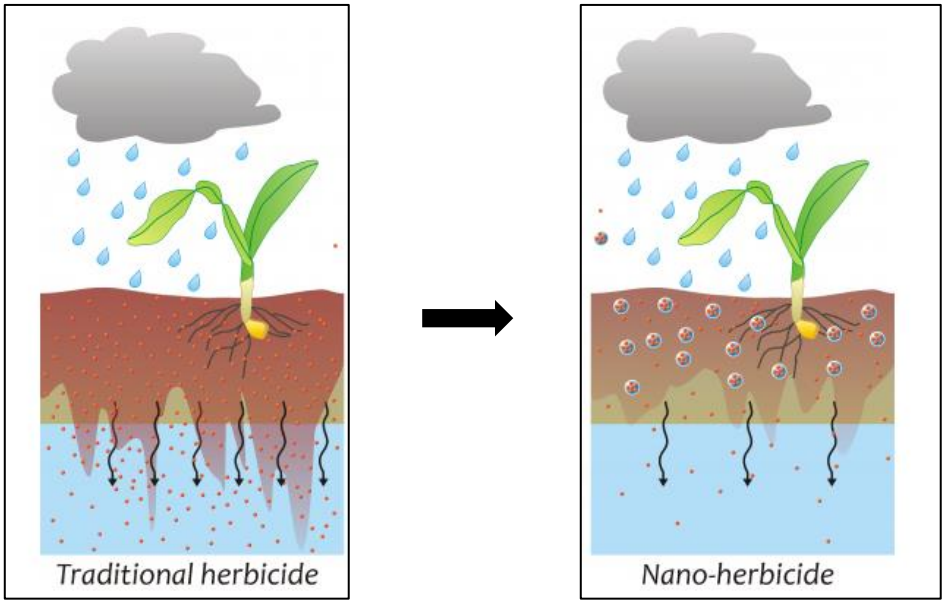

Figure 1: traditional herbicide behavior compared to a nano-herbicide. Source: Tosco, 2017.

This thesis focusses on the study of the transport behavior of the new nano-herbicide formulation, developed by the Groundwater Engineering group, which is meant to restrain the diffusion of the herbicide itself in the environment. The new formulation has been patented. This nano-herbicide has the potentialities of lowering the volatilization and loss of active ingredient during application, and of reducing the uncontrolled infiltration of the active ingredient after application in the subsoil, because of its composition. The formulation is made by absorbing the active ingredient of a common herbicide onto clay-based particles, which limit the free active ingredient mobility.

This thesis final aim is to simulate the behavior of the new developed formulations after application in a three dimensional scale and compare them with a conventional herbicide formulation. The goal is attained through the interpretation of one dimensional column tests, previously performed in the laboratory in saturated and unsaturated conditions, to three dimensional simulations. The work is carried out by using the software MNMS and Hydrus 1D for the one dimensional interpretation and HYDRUS for the three dimensional simulations.

In the first chapter an introduction to pesticides and nano-pesticides is described, highlighting the environmental fate of nano-formulations and their transport mechanisms. Also an overview on the theory of colloidal particles, their transport behaviors, their governing equations are presented as a background to better understand the following sections.
In the material and methods it is described how modelling the herbicide behavior in three dimensional scale is achieved starting from laboratory tests and data interpretation.
In the last chapter main results about the experimental data interpretation and the scenario modelling are reported together with the conclusions.

2. Background

2.1 Pesticides

According to the European Commission and the European Food and Safety Authority (EFSA), which among others deal with pesticides regulations and policies, a pesticide is “something that prevents, destroys, or controls a harmful organism ('pest') or disease, or protects plants or plant products during production, storage and transport” (European Commission, 2012).

The term 'pesticide’ is often used interchangeably with 'plant protection product'; however, pesticide is a broader term that also covers non plant/crop uses, for example biocides. The term includes herbicides, fungicides, insecticides, growth regulators, fungicides, acaricides, nematicides, molluscicides, rodenticides, repellents, rodenticides and biocides. Pesticides are usually composed of an active substance, which is the essential ingredient that enables the pesticide do its job, but may contain other components.

The use of conventional pesticides has been limited and revised in the past decades. In the European Union the marketing and use of plant protection products is regulated by many EU legislations. Active substances contained in plant protection products must be authorized before the placing on market and use through a process that involves the EFSA, the European Commission and Member States. A new substance is usually approved for 10 years, while the renewal of the authorization can be granted for up to 15 years (EFSA, 2018). On the ‘EU-pesticides portal’ it is possible to check for the banned substances. Every substance has different constraints based on its toxicity on human and animal health and the environment (European Commission, 2016). The goal of achieving a sustainable use of pesticides, reducing their risks and impacts on human health and the environment was promoted by the Directive 2009/128/EC by the European Union (European Parliament and Council, 2009).

Nano-pesticides have shown to have potentially better characteristics in term of selectivity, efficiency, and reduction of their overall environmental impact compared to the conventional ones (Balaure, et al., 2017).

Different types of nano-pesticides exists (Kah & Hofmann, 2014):

- Nano-emulsions
- Polymer-based nano-pesticides
- Hybrid nano-formulations
- Inorganic nano-particles associated with an organic active ingredient
- Inorganic nanoparticles as active ingredients

Nano-pesticides are currently a very interesting topic of research although field conditions tests and a thorough detailed assessment of the environmental impact of nano-pesticides compared to conventional ones are currently almost lacking in the literature (Kah, et al., 2018). Nano-formulations are considered promising because of, among others, the lower amount of active ingredient required during application which lowers the residues and the harmful effect on non-target organisms, such as humans, animals, micro-organisms and plants (Souza, et al., 2019). Other advantages of nano-pesticides against conventional ones are summarized in Figure 2, every type of nano-formulation exhibits different advantages.

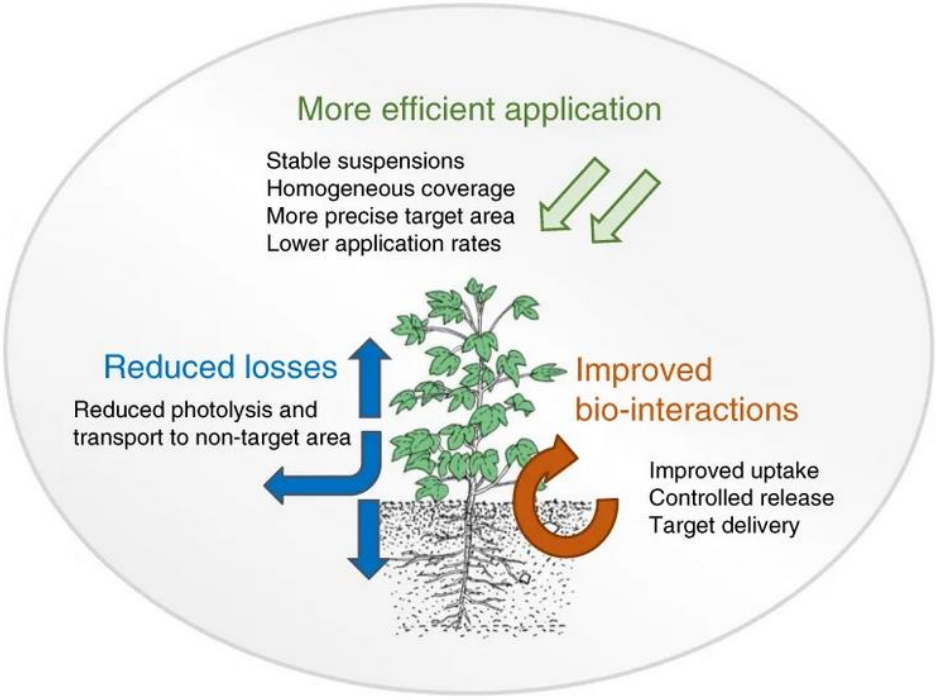

Figure 2: advantages of nano-pesticides against conventional analogues. Source: modified picture from Kah, et al. (2018)

2.1.1 Environmental fate of nano-pesticides

The environmental fate of a nano-formulation generally differs based on the formulation's constituents. In the last decades nano-formulations composed of active ingredients and a carrier have been studied. These kind of nano-formulations influence the mobility and the release-rate of the active ingredient in the environment. It is expected that nano-formulations can achieve slow release rate of the active ingredient and or protect it from premature degradation (Kah & Hofmann, 2014). In this thesis a nano-carrier, NC, loaded with an active ingredient, AI, is considered.

Kah & Hofmann (2014) report that the processes affecting the active ingredients depends on the transport behavior of the nano-formulation; which is affected by sorption and degradation. A drawback concerning the nano-formulation mobility is that the colloidal-facilitated transport of the active ingredient could be enhanced. The nano-carrier can indeed act as a mobile solid phase that increases the transport of the active ingredient (Ouyang, et al., 1996).

The transport in the subsoil of the nano-formulations can be described with three different models that consider the relation between the solute, that is the active ingredient, and the colloidal nano-carrier:

- classical solute transport models, when the release of AI from the NC occurs quickly relative to the transport time scale and the colloidal facilitated transport is neglected;
- solute transport and colloid transport, respectively describing the behavior of the dissolved AI and the behavior of the NC with the AI attached, when desorption occurs very slowly;
- transient behaviors over time, when release kinetics are needed to assess the transfer from attached to dissolved AI.

The last one is a thorough model to describe the transport behavior of the formulation of this study. However, in this project the solute transport and colloid transport models are assumed to be an acceptable approximation since the release of the AI from the NC used in this study occurs very slowly.

2.2 Colloidal particles

The nano-formulation behaves as a colloidal particles, therefore an overview on the theory of colloids is presented in this section.

The term 'colloidal' refers to "a state of subdivision, implying that the molecules or polymolecular particles dispersed in a medium have at least in one direction a dimension roughly between 1 nanometer and 1 micron" (IUPAC, 1997).

Different transport mechanisms of colloidal particles exists, governed by physical and physicochemical interactions. Colloidal particles transport occurs in the presence of:

- a solid matrix, also called the collector,
- a liquid phase, usually water,
- the colloidal particles.

2.2.1 Transport in the saturated porous medium

According to Kretzschmar (1999) the transport of colloids in porous media can be subdivided in two phases: one of deposition, and one of release from the collector, as shown in Figure 3. The deposition phase is the succession of the transport of colloidal particles to the collector and the following attachment of colloidal particles to the collector surface.

The first phase, the transport to the collector, results in colloid-collector collision. This phase is controlled by the single-collector contact efficiency, which describes the mechanisms taking the colloid to the collector, and is defined in details in Part A of the Appendix. Physical factors, such as size and density of the colloidal particles, accessible surface area for the deposition, pore structure and flow velocity govern the transport phase kinetics.

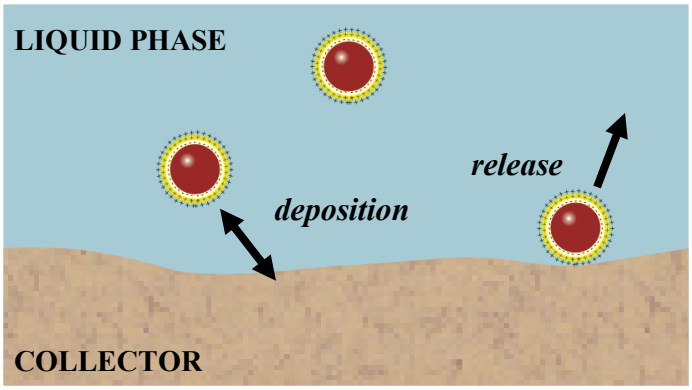

Figure 3: detail about the deposition and release phase of the colloidal particles transport. Source: modified image from the conference slides Tosco, et al. (2016).

On the other hand, the kinetics of the attachment is governed by surface interactions forces, such as the ones described by the DLVO theory, which are described in the Appendi. Surface interactions are the inter-particle forces between colloidal particles and between particles and collector, which among others are affected by the solution and surface chemistry. The collision phase is governed by the attachment or collision efficiency, α, that represents the amount of colloid-matrix collisions that results in attachment of the colloidal particle on the collector (Kretzschmar, et al., 1999).

Considering an homogeneous, water saturated porous medium, colloidal particles under steady state flow conditions are transported according to advection and dispersion, and to the particle-particle and particle-collector interactions. Assuming that the volume of colloids is negligible compared to the pore volume, colloidal particles transport can be modelled in saturated porous media through a modified advection-dispersion equation, and with an exchange term that includes particles interactions with the solid and liquid phase. The following equation represents the mass balance of the particles suspended in the liquid phase (Tosco, et al., 2018):

$$n\frac{\partial c}{\partial t} + \rho\frac{\partial s}{\partial t} = -v\frac{\partial c}{\partial x} + nD\frac{\partial^2 c}{\partial x^2} \quad (1)$$

where:

- n is the porous medium effective porosity [-],

- c is the colloid concentration in the liquid phase [M L^{-3}],
- ρ is the bulk density of the solid matrix [M L^{-3}],
- s is the colloid concentration in the solid phase [-],
- v is the Darcy's velocity [L T^{-1}],
- x is space [L],
- t is time [T],
- D is the dispersion coefficient [L^2T^{-1}] define as:

$$D = \alpha v_e \tag{2}$$

where:

- α is the porous medium dispersivity [L],
- v_e is the effective velocity [L T^{-1}], defined as:

$$v_e = \frac{v}{n} \tag{3}$$

The mass balance of the particles attached to the solid phase is represented by a second equation as a general non-equilibrium term:

$$\rho \frac{\partial s}{\partial t} = f(c, s) \tag{4}$$

This term differs according to the colloidal particles attachment behaviors.

When different interactions behaviors with the colloidal particles are considered, two or more interaction sites are included, by adding a term for each interaction site (Tosco & Sethi, 2009):

$$f(c, s) = \rho \frac{\partial s_1}{\partial t} + \rho \frac{\partial s_2}{\partial t} + \cdots \tag{5}$$

2.2.2 Transport in the unsaturated porous medium

In unsaturated porous media, a gas phase is contained in addition to the liquid and solid phases. This is the situation for unsaturated soils and the underlying vadose zones. The ability of a soil to retain or transmit water and its dissolved constituents can be assessed by knowing the hydraulic properties of unsaturated soils. These are the volumetric water content and the unsaturated hydraulic conductivity, which are non-linear parameters that depends on the pressure head. These properties are necessary when using mathematical models to study the water flow or solute transport processes in the subsurface.

The volumetric water content, θ [-], that depends on the pressure head, gives the soil water retention curve. This describes the relation between the water content and the available energy of water at a given point in the soil. In case of unsaturated conditions, the pressure head, that represents the difference of pressures between the air and liquid phases, assumes negative values relative to free water, as water undergoes capillary forces in the pores and adsorption on the solid phase. Conversely it assumes positive values in saturated conditions.

The van Genuchten model (van Genuchten & Pechepsky, 2011) uses the following equations to describe the soil water retention curve and therefore the soil hydraulic parameters (van Genuchten, 1980):

$$\theta(h) = \theta_r + \frac{\theta_s - \theta_r}{[1 + |\alpha h|^n]^m} \qquad h < 0 \tag{6}$$

$$\theta(h) = \theta_s \qquad h > 0 \tag{7}$$

where:

- h is the pressure head [L]
- θ_s is the saturated water content [-]
- θ_r is the residual water content [-]

- α is the inverse of the air-entry value or bubbling pressure [L^{-1}]
- *m, n* are empirical parameters [-], related to each other according to:

$$m = 1 - \frac{1}{n} \qquad n > 1 \tag{8}$$

Typical soil water retention curves for different soils are shown in Figure 4. The three curves are typical for relatively coarse-textured materials, such as sand and loamy sand, for medium-textured, like loam and sandy loam, and for fine-textured materials, as for example clay loam, silty loam, or clay. This curve is usually determined by a gradual desaturation of a saturated soil, by applying higher suctions.

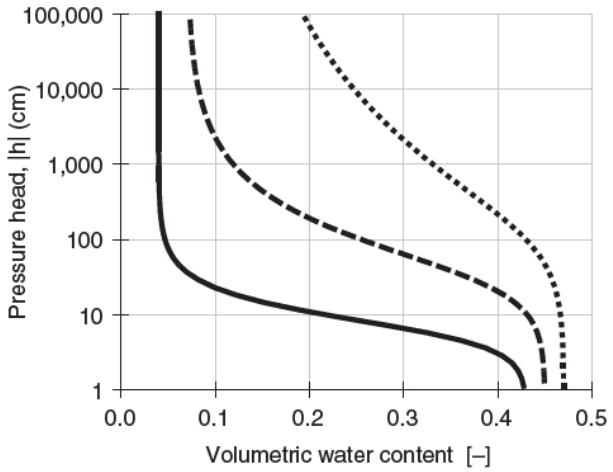

Figure 4: typical soil water retention curves for relatively coarse- (solid line), medium- (dashed line), and fine-textured (dotted line) soils. Source: van Genuchten & Pechepsky (2011).

The water content values lay between a maximum value, the saturated water content, θ_s, and a minimum value, the residual water content, θ_r. At first approximation, the porosity can be estimated as the saturated water content of soils, although in reality the water content is slightly smaller due to entrapped and dissolved air (van Genuchten, et al., 1991). The residual water

content instead is usually higher than zero, because of the water adsorbed on the soil surface (van Genuchten & Pechepsky, 2011).

The hydraulic conductivity is an index of the quantity of water that can be transmitted by the soil. It is a function of the pore-size distribution of the medium, the tortuosity, the shape, the roughness, and the degree of interconnectedness of the pores. In unsaturated soils, it also depends on the water pressure head. Its value decreases with decreasing water content, since more space is occupied by air and as the flow paths are more tortuous, the drag forces between the solid and liquid phases become higher.

The hydraulic conductivity function which depends on the pressure head, based on soil water retention parameters, can be described as follow:

$$K(h) = K_s \, S_e^l \, [1 - (1 - S_e^{1/m})^m]^2 \tag{9}$$

where, besides the previously defined terms:

- K_s is the saturated hydraulic conductivity [LT^{-1}],
- l is a parameter accounting for the pore-connectivity, and assumed to be 0.5 for many soils (Mualem, 1976),
- S_e is the effective saturation [-], defined as:

$$S_e = \frac{\theta - \theta_r}{\theta_s - \theta_r} \tag{10}$$

2.2.2.1 Water flow and solute transport

Predictive models to describe the water flow in unsaturated soil are usually based on the Richards equation, valid for one-dimensional vertical flow (Richards, 1931):

$$\frac{\partial \theta(h)}{\partial t} = \frac{\partial}{\partial z}\left[K(h)\frac{\partial h}{\partial z} - K(h)\right] \tag{11}$$

where:

- θ is the volumetric water content [L^3L^{-3}],
- h is the water pressure head [L],
- t is time [T],
- z is the soil depth [L], which is positive when directed downward,
- $K(h)$ is the unsaturated soil hydraulic conductivity function [LT^{-1}].

Similar equations can be predicted for multidimensional flow. The volumetric water content function and the unsaturated soil hydraulic conductivity are in general highly nonlinear functions, that have been previously described in equation 6 and equation 9 .

The colloidal particles transport in unsaturated soils can be described by the 'Attachment-Detachment Model' or 'Two Kinetic Sites Model', which is a solute transport model (Šimůnek, et al., 2013).

It is assumed that interactions between the solid and liquid phases may be described by nonlinear non-equilibrium equations, while interactions between the liquid and gaseous phases are assumed to be linear and instantaneous. Moreover it is assumed that the solutes are transported by advection and dispersion in the liquid phase, and by diffusion in the gas phase.

The mass balance of unsaturated soils considering colloidal particles transport can be described by a modified version of the advection-dispersion equation (Šimůnek, et al., 2013):

$$\frac{\partial \theta c}{\partial t} + \rho \frac{\partial s_e}{\partial t} + \rho \frac{\partial s_1}{\partial t} + \rho \frac{\partial s_2}{\partial t} = \frac{\partial}{\partial x}\left(\theta D \frac{\partial c}{\partial x}\right) - \frac{\partial vc}{\partial x} - \mu_w \theta c - \mu_s \rho (s_e + s_1 + s_2) \qquad (12)$$

where:

- c is the colloid concentration in the liquid phase [M L^{-3}],
- θ is the volumetric water content [L^3L^{-3}],
- s is the solid phase (colloid, virus, bacteria) concentration in the solid phase [MM^{-1}],
- v is the Darcy's velocity [L T^{-1}],
- D is the dispersion coefficient [L^2T^{-1}], defined in equation 2,
- ρ is the bulk density of the solid matrix [M L^{-3}],
- subscripts *e*, 1, and 2 respectively represent equilibrium and two kinetic sorption sites,
- μ_w considers the inactivation and degradation processes in the liquid phase [T^{-1}],
- μ_s represents inactivation and degradation processes in the solid phase [T^{-1}].

2.2.3 Deposition mechanisms

The deposition phase has classically been described by the classical filtration theory (CFT). This theory describes the initial removal of particles from the suspension following an exponential decrease in suspended colloid concentration with travel distance. This is described by a pseudo first-order kinetics rate-flow, which does not consider the possible detachment of colloids from the medium (Elimelech, et al., 1995). The CFT model is only used for the early stage of the deposition. The clean bed hypothesis is valid, which means that the detached particles are assumed negligible and blocking and ripening not relevant. This is also known as a linear irreversible model. The model is described by the following equation:

$$\rho \frac{\partial s}{\partial t} = k_a \theta c \tag{13}$$

where the attachment coefficient, k_a, is calculated according to the filtration theory with a quasi-empirical formulation which considers colloidal particles attachment to the collector due to diffusion, interception and gravitational sedimentation (Logan, et al., 1995):

$$k_a = \frac{3(1-\theta)}{2d_c} \eta \alpha v_e \tag{14}$$

where:

- d_c is the diameter of the sand grains [L],
- α is the attachment efficiency, which represents the ratio of particles that stick to a collector to the rate they strike the collector [-],
- v_e is the pore water velocity [LT^{-1}],
- η is the single-collector efficiency [-] as defined in Appendi.

The filtration theory is useful to describe the initial kinetics of colloidal particles deposition onto the porous medium, however the deposition rate can increase or decrease after that a non-

negligible amount of colloids have been deposited on the collector, since the presence of deposited particles may affect the deposition of suspended ones by modifying particle-collector interactions. Moreover, the colloid filtration theory was developed under the assumption of no repulsion between particles and collector, which may not be true for the majority of colloidal particles found in natural subsurface systems (e.g. clay particles, bacteria etc.). Therefore depending on the specific particle-particle and particle-collector interactions, other models can be used to describe the deposition behavior:

- linear reversible attachment,
- blocking,
- ripening.

It is worth mentioning that all the deposition mechanisms are highly influenced by the chemistry of the solution. Also the ionic strength of the solution influences the total interaction potential. Higher ionic strength contributes to higher attraction between particles or particle-collector, because the ionic strength reduces the electrical repulsive interactions.

The possible behaviors are described with their equation. Notice that the equations are written in relation to the volumetric water content θ, which in first assumption is considered to be the same as the porosity, n, in the case of saturated soils. These equations are valid both for the saturated and the unsaturated conditions.

Reversible attachment

It occurs when particle-particle and particle-collector energies are similar. Deposited particles do not affect the suspended ones as shown in Figure 4.

The function is similar to the irreversible model, that is described by the clean bed filtration theory, but in this case the detachment is considered:

$$\rho \frac{\partial s}{\partial t} = \theta k_a \Psi c - k_d \rho s \tag{15}$$

where:

- k_a is the first-order attachment coefficient [T^{-1}],
- k_d is the first-order detachment coefficient [T^{-1}],
- Ψ is a dimensionless colloidal particles retention function [-], which varies according to the colloids behavior, as defined in the following lines.

Blocking

Also known as excluded area effect, it occurs when colloid-colloid attachment is unfavorable and as a consequence the decrease in the attachment rate evolves until the maximum colloid concentration, s_{max} , on the collector is reached. A representation of blocking phenomenon can be seen in Figure 6. The blocking phenomenon, that leads to a reduction of the attachment rate in time due to filling of the available sorption surface, is taken into account by considering a Langmuirian dynamics equation, which described the Ψ function that decreases with the increase of the colloidal particles mass retention (Adamczyk, et al., 1994):

$$\Psi = \frac{s_{max} - s}{s_{max}} = 1 - \frac{s}{s_{max}} \tag{16}$$

where s_{max} [MM^{-1}] is the maximum solid phase concentration retainable on the solid phase at given chemical conditions.

Ripening

It occurs when particle-particle interactions are favorable, that is when the interaction energies are attractive. In this condition deposited colloids attract the suspended ones, resulting in a gradual increase in the attachment rate, until the clogging of the porous medium. A graphical representation of the ripening phenomenon is shown in Figure 7.

The ripening phenomenon is described by a function that increases with the increasing retained colloidal particles (Šimůnek, et al., 2013):

$$\Psi = \max(1, s^{Smax}) \tag{17}$$

Another way of defining ripening is the following (Bianco, et al., 2018):

$$\Psi = 1 + A_{rip} S^{\beta_{rip}} \tag{18}$$

where A_{rip} [-] and β_{rip} [-] are the ripening coefficients, with $A_{rip} > 0$ and $\beta_{rip} > 0$, meaning that the deposition rate increases with increasing concentration of attached particles.

Linear reversible

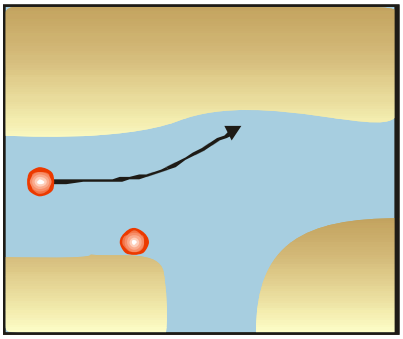

Figure 5: linear reversible attachment model of the transport of colloidal particles. Source: conference slides Tosco, et al. (2016).

Blocking

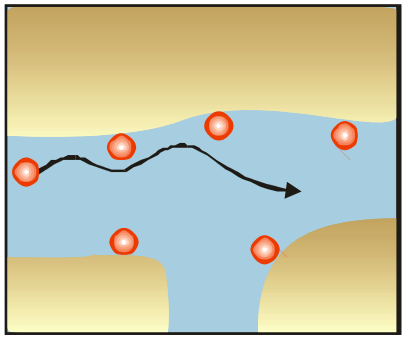

Figure 6: the blocking effect on the transport of colloidal particles. Source: conference slides Tosco, et al. (2016).

Ripening

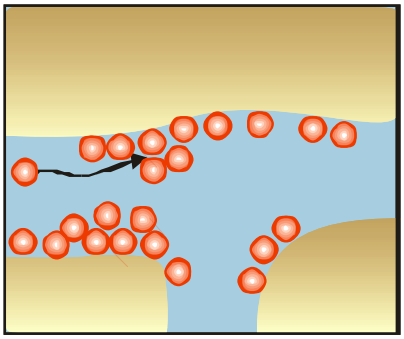

Figure 7: the ripening effect on the transport of colloidal particles. Source: conference slides Tosco, et al. (2016).

3. Materials and Methods

In order to study the transport of the formulations in the soil, laboratory tests were performed injecting the nano-herbicide formulation dispersed in different solutions (NaCl solution and tap water) in sand-packed columns, in both saturated and unsaturated conditions as described in the unpublished master's thesis of Granetto (2018) and Re (2019). The data obtained in the tests were processed and interpreted using the software MNMs (Tosco, et al., 2018) for saturated conditions, and Hydrus 1D (Šimůnek, et al., 2013) for unsaturated conditions. The experimental results were modelled using equations 1, 11, 12 and 15, and the colloid transport parameters obtained via least-square fitting were then used for the three dimensional transport simulations in HYDRUS (Šimůnek, et al., 2012). In Figure 8 a schematic representation of the methodology used, the output at each step and the software used are shown.

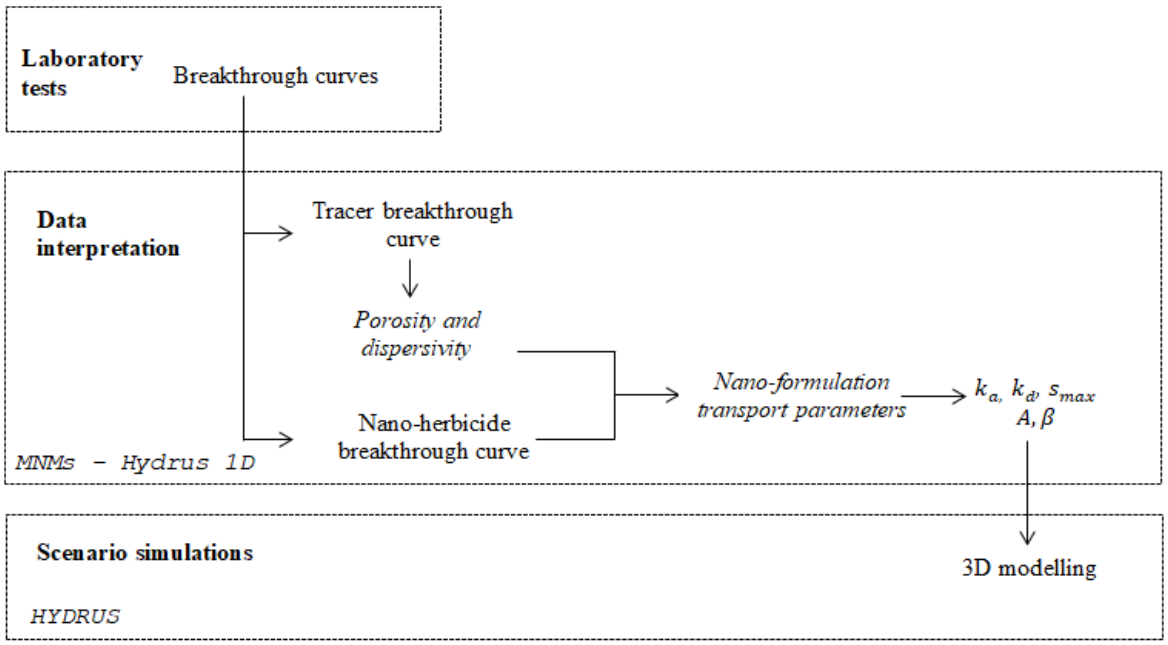

Figure 8: schematic representation of the methodology with the estimated parameters and the software used.

During the laboratory tests breakthrough curves were obtained from the tracer test and from the nano-herbicide injection. From the tracer breakthrough curve, the porosity and dispersivity

values are estimated and used as inputs when interpreting the breakthrough curves of the formulation transport. From the data interpretation of the nano-herbicide injection, the following hydrodynamic transport parameters are estimated:

- the attachment rate, k_a [1/T],
- the detachment rate, k_d [1/T],
- the maximum solid phase concentration, s_{max} [-], when blocking exists,
- the ripening coefficients, A [-] and β [-], when ripening exists.

3.1 Laboratory tests set up

3.1.1 Formulations

A patent has been filed on the nano-herbicide formulation at issue.
The nano-herbicide is composed of the active ingredient, adsorbed on a nanocarrier. The active ingredient is the herbicide Dicamba, 3,6-dichloro-2-methoxybenzoic acid; an herbicide used for maize, sorghum and wheat crops. The carrier is constituted by Montmorillonite clay. Some experiments are also carried out using the formulation prepared with a biodegradable coating composed of carboxymethyl cellulose, a polymer, also known as CMC. Therefore the formulations used in the laboratory are of two types:

A. formulation without coating,
B. formulation with coating.

For each test, one of the two types of formulations was injected in the sand-packed column and was flushed using different solutions, including deionized water, 30 mM NaCl solution, and tap water (as described in the next paragraph).
In some tests the pH of NaCl solutions was adjusted to match the pH of tap water in order to evaluate if the particles behavior in the transport is mostly affected by the pH or by other properties of tap water, such as the salts concentration and type and its ionic strength. In order to change the pH values, 2.5M NaOH were added to the solution.

3.1.2 Column tests

Column tracer tests and column transport tests were performed both for the saturated and the unsaturated conditions following the same procedures.

Tracer tests procedure included:

- Pre-flushing with deionized water
- Tracer injection with 30mM NaCl

Column transport tests were performed including different steps:

- Pre-flushing with particle-free solution
- Formulation injection (i.e. stock nano-herbicide formulation diluted to 0.9 mmol/l)
- Flushing with particle-free solution

The procedure of column transport tests is the same for saturated and unsaturated conditions and is described in Table 1.

Table 1: particles injection laboratory procedure using 30 mM NaCl or tap water and duration of each step.

Procedure	Injection	Pore volumes
Pre-flushing	DIW	2
Conditioning	30 mM NaCl / tap water	5
Particles injection	formulation	5
1st flushing	30 mM NaCl / tap water	5
2nd flushing	DIW	10

The tracer and particles breakthrough concentration at the outlet was monitored using a UV-vis spectrophotometer (Specord S600, Analytik Jena, Germany); the results were modeled to estimate the solute transport parameters (namely, porosity and dispersivity) and colloid transport parameters (namely, attachment and detachment rate) for each test.

Saturated conditions

In the laboratory the experiment was set up using a Plexiglas column (1.6 cm diameter, 11.5 ± 0.05 cm long), filled with 36.5 g of medium sand (Dorsilit 8, Dorfner, Germany). For each test a tracer test was performed to determine the hydrodynamic parameters of the porous medium injecting a 30 mM NaCl solution. The discharge rate was kept constant for the entire test and it was 1.94 x10^{-8} m^3/s.

Unsaturated conditions

Tests in unsaturated conditions were performed at a constant discharge rate of 1.46 x10^{-8} m^3/s. Plexiglas columns were filled with 55 g of sand. The columns have a diameter of 1.6 cm and a length of ca 17 cm.

Before starting the particles injection step, two tracer tests with NaCl in saturated and unsaturated conditions were performed for every column test. When performing the unsaturated column tests, a tracer is first used through the saturated column, then the column is desaturated and another tracer test is done in the desaturated sand column. After these processes the nano-formulation is injected. The procedure is described in Figure 9.

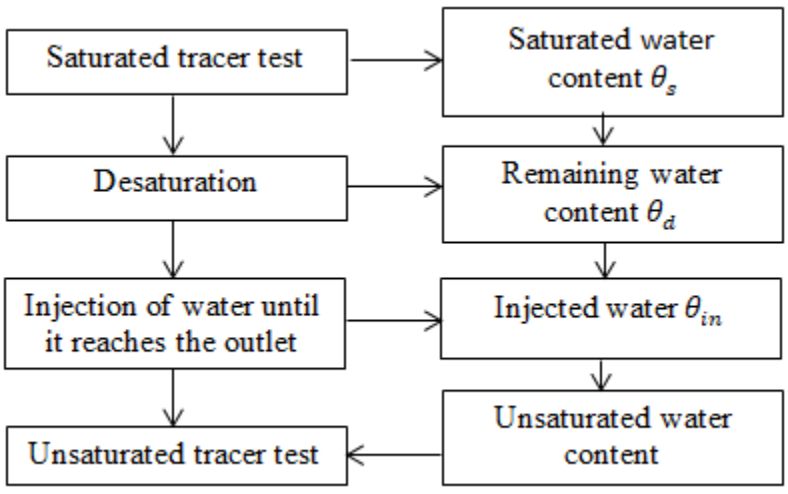

Figure 9: procedure used before the particles injection in unsaturated conditions and parameters obtained at each step.

When the column was desaturated, the weight of the water released by gravity was measured. Moreover, water was injected until it was coming out of the outlet and measured. At that time the pump was connected. The time of the beginning of the injection, t_1, and when water reached the outlet, t_2, were recorded.

This is done in order to know the unsaturated water content before the formulation is injected. The unsaturated water content is given by the sum of the water remaining in the column when the column is desaturated (θ_d), calculated by:

$$\theta_d = \frac{\left(nV - \frac{m}{d}\right)}{V} \tag{19}$$

where

- n is the porosity of the sand column [-],
- V is the volume of the sand column [L^3],
- m is the weight of released water after desaturation [M],
- d is the water density [M/ L^3],

and the water injected in the column, θ_{in}, calculated as shown in the following equation:

$$\theta_{in} = \frac{Q \cdot (t_2 - t_1)}{V} \tag{20}$$

where:

- Q is the discharge rate [L^3/T],
- t_1 and t_2 are the recorded times, as described in the text [T].

To sum up 6 different test types were performed for the saturated sand-packed column and 6 for the unsaturated one as shown in Table 2. The 6 test types are the following:

- Test with coating in NaCl
- Test with coating in tap water
- Test with coating in NaCl at modified pH
- Test with no coating in NaCl
- Test with no coating in tap water
- Test with no coating in NaCl at modified pH

An extra test was performed injecting the carrier without active ingredient in saturated conditions, as a reference to compare mobility of the nano-formulations.

Table 2: the different types of tests performed.

Column conditions	Injected formulation	Solution
Saturated Unsaturated	With coating No coating	NaCl Tap water NaCl modified pH

3.2 Data interpretation

The tracer breakthrough curves of the laboratory tests are used as inputs for the test interpretation from which the porosity and the dispersivity are estimated. Those two values are used as inputs in the transport interpretations from which the transport parameters are estimated as shown in Figure 10. The numerical tools are run in inverse mode since parameters are estimated from experimental data. Colloidal particles breakthrough curves are used as inputs in the software to study the colloidal particles transport behaviors and to estimate their transport parameters.

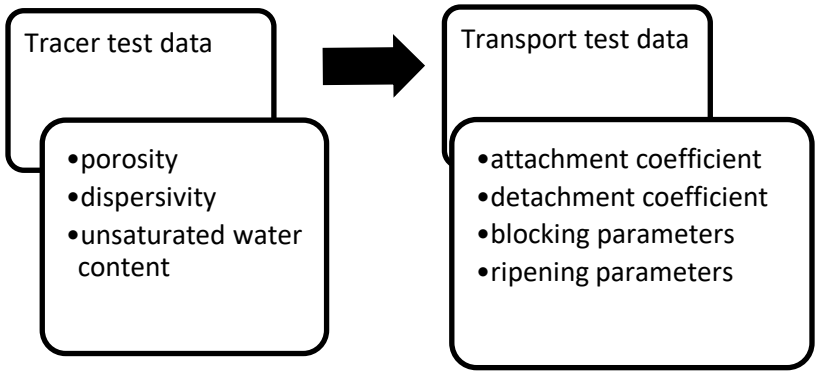

Figure 10: laboratory tests data and the estimated parameters after their interpretation.

Beside the saturated tracer tests, interpreted both with MNMs and Hydrus 1D, the tracer tests for the unsaturated case were entirely interpreted in Hydrus 1D. MNMs is then used for the transport data interpretation of saturated columns, and Hydrus 1D for the one of unsaturated columns.

3.2.1 Assumptions

The formulation transport interpretation is performed studying the behavior of the nano-herbicide formulation in the porous matrix. It is assumed that the nano-herbicide behaves as a colloidal particle. The colloidal facilitated transport is not considered in this study, although it may influence a lot on the diffusion of the formulation in the soil.

When performing the unsaturated column tests interpretation, the dispersivity of the active ingredient, Dicamba is assumed to have the same value as the dispersivity of the tracer in unsaturated conditions, although this may be a simplification since Dicamba is adsorbed on clay particles at the beginning and therefore would have a different dispersivity value.
Degradation of the active ingredient is not considered.

3.2.2 The saturated tests interpretation

Tracer tests

MNMs is used for the data interpretation in saturated conditions (GW@POLITO, 2014).
MNMs, Micro- and Nanoparticles transport, filtration and clogging Model – Suite, is a numerical tool useful to analyze laboratory column transport tests results in saturated conditions of colloidal particles and solutes (Bianco, et al., 2018). MNMs is the evolution and combination of two previous software: MNM1D (Tosco & Sethi, 2009) and E-MNM1D (Tosco & Sethi, 2010).

MNMs allows to calculate in direct and inverse mode the interaction energy profiles using the DLVO and extended DLVO theory, the single collector efficiency and simulate the transport of dissolved species and colloidal particles in 1D geometry and in radial geometry.

MNMs estimates the porosity and dispersivity by using an analytical solution which solves the water flow and solute transport equations (equations 1 and equation 15). The simulation is run in an inverse mode. In the software, the inputs for each tracer test are:

- the system properties:
  - the column length, which varies from test to test, but it is usually around 0.11 m,
  - the radius of the column, which is 0.008 m,

- the discharge rate, which is 1.94 x10^{-08} m^3/s,
- the density of the sand, which is 2630 kg/m^3,

- the interaction parameters:
  - the initial concentration in the liquid phase, which is set as 0 kg/m^3,
  - the duration of the injection, which varies from test to test,
  - the tracer concentration in the liquid phase, which is 1.753 kg/m^3,

- the breakthrough curve data as recorded at the outlet.

The boundary condition chosen for the inlet is the 1st type, known as Dirichlet's boundary condition. This boundary condition in the solute transport partial differential equation solution, specify the value that the solution has to take at the inlet of the domain, in this case concentration values.

Nano-herbicide transport tests

MNMs is used for the transport interpretation in saturated conditions. The expected transport behavior is selected before running the calculations, the user can select between one or two active sites. In this study two sites are chosen one for the linear irreversible behavior, the other for ripening or blocking.

Beside the system properties, which are the same as in the tracer test simulation, the following are given as inputs:

- porosity [-], estimated from the tracer test interpretation,
- dispersivity [L], estimated from the tracer test interpretation,
- initial salt concentration in the liquid phase: 30 mM,
- stress period duration of the colloidal particles injection,
- stress period duration of the '1st flushing' step when NaCl or water is used.
- ionic strength of the '1st flushing' injected solute:
  - tap water ionic strength: 13 mM
  - NaCl ionic strength: 30 mM

- the particles concentration in the liquid phase: 0.9 kg/m^3,

Since the detachment rate is very low and almost irrelevant in the case of a linear irreversible behavior, it is set to a very low value, 1x10^{-11} 1/s, and not estimated. A first type boundary condition is selected for the inlet.

The estimated values are generally accepted when the R-square value is equal or above 95%. If this percentage is not reached a manual calibration is performed in order to obtain a better fitting of the predicted curve on the experimental data. There are a few cases where lower R-square values are accepted when the fitting curve is graphically suitable over the experimental data and the lower R-square values are due to very spread experimental values.

3.2.3 The unsaturated tests interpretation

Tracer tests

Hydrus 1D is used to interpret the saturated column tracer test, and the unsaturated column tracer test and colloidal particles transport in unsaturated conditions. Hydrus 1D is a public domain software package that allows to simulate and analyze water, heat, and solute transport in unsaturated, partially saturated and fully saturated porous media (Simunek, et al., 2019).

In the case of unsaturated conditions, two tracer tests were performed. The interpretation of the first, in saturated condition, gives an estimation of the saturated water content, necessary to analytically calculate the water content in the column after desaturation, before the unsaturated tracer test. This water content value is then used in the unsaturated tracer test interpretation, in which the dispersivity and the unsaturated water content are estimated. These two parameters are then used for the particles transport test interpretation.

The provided parameters in the pre-processing phase are the following:

- geometry information:
  - the column length,

- soil hydraulic parameters, the van Genuchten-Mualen model is selected as soil hydraulic model:
  - the hydraulic conductivity, k, for the saturated test is calculated according to the Darcy's law (Di Molfetta & Sethi, 2012):

$$k = -\frac{Q}{A} \cdot \frac{dl}{dh} \tag{21}$$

where:

- Q is the discharge rate, 1.46 x10^{-8} m^3/s,
- A is the round section of the column [L^2],
- dl/dh [-] is the inverse of the hydraulic gradient, which is 1 in this case,

  - n, α and l are parameters describing the soil water retention curve in unsaturated conditions. In the case of saturated conditions, they are respectively assigned the values 1 and 0 for the other two, as they are not relevant to describe the saturated soil hydraulic properties. In the case of unsaturated conditions the values provided in the soil catalog on the software for sand are used. Those are:

    α = 3.53 1/m

    n = 3.1798

    l = 0.5
  - θ_s, the saturated soil water content, that is estimated,

- water flow boundary conditions:
  - upper BC: constant flux of 9.68 x10^{-5} m/s,
  - lower BC: constant pressure head. The initial pressure head condition which is positive for the saturated case and negative for the unsaturated case,

- solute transport:
  - Galerkin Finite Elements space weighting scheme is selected,
  - the tracer injection duration, which varies from test to test,

- solute transport boundary condition
    - upper BC: concentration BC of 1.753, which is the concentration of the solute (NaCl) of the injected water,
    - lower BC: zero concentration gradient,

- data for the inverse solution:
    - breakthrough curves data at the end of the column,
    - initial water content for the unsaturated interpretation.

Nano-herbicide transport tests

The conceptual model is the same as in the case of the tracer test. As a matter of fact, both are interpreted using a solute transport model. However this time, the solute transport in Hydrus 1D can be described by the 'Attachment-Detachment Model' or 'Two Kinetic Sites Model', in order to consider the colloidal particles transport parameters. The water content given as input is the one estimated from the tracer test.

3.3 Scenario simulations

Three dimensional scenario simulations are performed in HYDRUS. HYDRUS is a finite element model used to simulate two- and three-dimensional movement of water, heat, and multiple solutes in variably saturated media. The software allows to simulate colloids transport through the attachment/detachment theory, as in the Hydrus 1D software.

The same scenarios are run to compare the behavior of three herbicides in the solid medium. The considered solutions are:

- a conventional herbicide application,
- the nano-herbicide formulation with coating,
- the nano-herbicide formulation without coating.

The transport parameters estimated in the data interpretation step in Hydrus 1D of the tests that have shown better results in term of fitting and clear breakthrough curve of the colloids, are used as inputs in HYDRUS. The conventional herbicide in HYDRUS is treated as a general solute, the nano-herbicide formulations instead are modelled as colloidal particles with the attachment/detachment model.

The scenarios are purely theoretical and the model is not calibrated, the simulations represent a preliminary study to be further implemented with more realistic conditions and calibrated with site-specific data. The simulated scenarios are the following:

- Scenario A: application of the herbicide and simulation of 12 h
- Scenario B: application of the herbicide and 6 hours of heavy rain
- Scenario C: application of the herbicide and irrigation

Results are registered at different observation points (specified in Part B of the Appendix), added to the domain in order to build a concentration profile with depth. The depth vs. concentration curves are obtained by interpolating the results of the added observation points.

3.3.1 Assumptions and limitations

The model is built assuming that:

- the herbicide application is instantaneous and occurs at the same moment on the field surface,
- the herbicide does not undergo any degradation process,
- the transport occurs in a sandy material, this is because the transport parameters are estimated from a sand column,
- no evapotranspiration is considered,
- irrigation is simulated with a 10 cm pressure head,
- heavy rain has an intensity of 20 mm/h (Arpa Piemonte, 2019),
- the aquifer is in steady state conditions,
- the herbicide is applied through a constant flux, calculated incrementing the velocity of application by a factor of 100, which takes into account the possible multiple application, as the herbicide may touch a specific area more than once. It is know that the tractor moves at a speed of 100 m/min and its action range is a surface of 10x0.5m. The herbicide is applied at a discharge rate of 1.5 l/min (0.0015 m^3/min). In one minute the tractor has covered an area of 100x10m, so the flux application is of 1,5 x 10^{-6} m/min. The set flux is 1,5 x 10^{-4} m/min,
- blocking effect is not considered in the nano-herbicide transport as it is assessed as negligible.

These are strong assumptions that can be very different from real situations. Soil in reality is very heterogeneous and very different behaviors can be expected compared to the one seen in the homogenous sandy material.

The conceptual model, being a simplification of a real life situation, carries some inherent limitations.

3.3.2 Conceptual model

Two different 3D geometries are built in HYDRUS and are shown in Figure 11:

1. a simple cubic geometry,
2. a field that contains a squared section where the herbicide is applied and an aquifer located 1 m underneath the field.

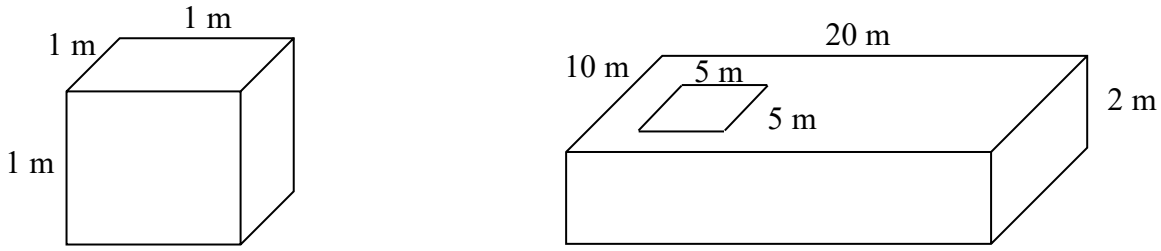

Figure 11: the two different geometries, not in scale.

The cubic geometry can be thought as a part of the crop field simulated in the second geometry. For both the geometries a constant flux boundary condition (BC) is assigned to the surface when the herbicide is injected, an atmospheric BC is assigned when simulating the rain and a constant pressure head for the irrigation. A free drainage BC is assigned to the bottom of the simple geometry. The assigned boundary conditions are shown in the schematic representation in Figure 12. For the second geometry the model is build considering an hydraulic gradient of 50 cm and consequently a constant flux of 0.011 cm/min (calculated with the Darcy's law) for the aquifer.

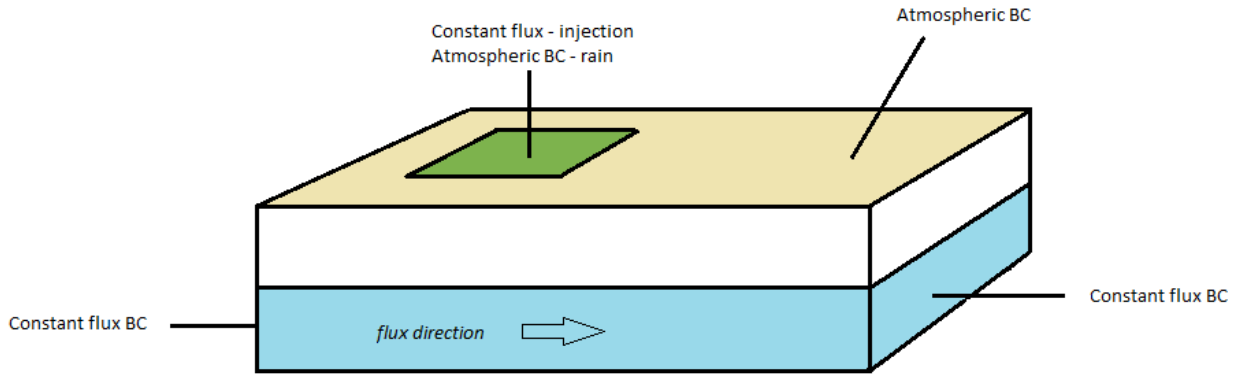

Figure 12: conceptual representation of the model with the assigned boundary conditions, not in scale.

Below there is a summary of the simulations performed in HYDRUS, every simulation is run for each of the three formulations. The instantaneous application simulation results are used as inputs for the others, as well as the steady state simulation for the second geometry.

For the cubic geometry:

- instantaneous application of the herbicide,
- scenario A, B, and C.

For the geometry with the aquifer:

- steady state water flow simulation,
- instantaneous application of the herbicide,
- scenario B.

4. Results and discussion

4.1 Column tests data interpretation

4.1.1 Saturated conditions

Tracer tests

The results of the tracer test interpretation in saturated conditions performed both in MNMs and Hydrus1D are reported and discussed in this section. The estimated porosity and dispersivity values are shown in Table 3, where also the R-square value is shown. For simplicity, although the tracer test is always performed injecting 30 mM NaCl, the results are subdivided based on the procedure used after the tracer test was performed. The test name is assigned based on the solution used for the test, tap stands for tap water.

Table 3: saturated column tests interpretation using MNMs and Hydrus-1D.

Formulation	Test name	Effective porosity [-]		Dispersivity [m]		R^2 MNMs	R^2 Hydrus -1D
		MNMs	Hydrus-1D	MNMs	Hydrus-1D		
No coating	NaCl 1	0.307	0.306	1.62×10^{-04}	1.62×10^{-04}	0.96	0.97
	NaCl 2	0.298	0.295	1.83×10^{-04}	1.81×10^{-04}	0.98	0.98
	Tap 1	0.382	0.384	1.44×10^{-04}	1.40×10^{-04}	0.99	0.99
	NaCl mod pH 1	0.371	0.374	1.34×10^{-04}	1.28×10^{-04}	0.70	0.80
With coating	NaCl 3	0.327	0.327	1.81×10^{-04}	1.78×10^{-04}	0.97	0.98
	NaCl 4	0.341	0.343	3.11×10^{-04}	3.07×10^{-04}	0.94	0.94
	Tap 2	0.441	0.441	2.75×10^{-04}	2.77×10^{-04}	0.96	0.98
	NaCl mod pH 2	0.210	0.212	7.61×10^{-04}	7.45×10^{-04}	0.91	0.91
Clay	NaCl	0.391	0.391	4.17×10^{-04}	4.22×10^{-04}	0.94	0.95

The porosity values are the same if approximated to two decimal places, while the dispersivity values show a higher degree of variation. However they are always on the same order of magnitude. Except for two cases, the dispersivity values are slightly lower when estimated through Hydrus-1D. The different values can be explained considering the different solutions implemented in the two software: MNMs calculates an analytical solution while Hydrus-1D estimates the parameters through a numerical implementation. Moreover there are some differences in the set-up of the two tools. In Hydrus 1D the initial pressure head is explicitly imposed while in MNMs is not. The saturated water content, that is assumed to be equal to the porosity, directly depends on the pressure head in Hydrus through the Richards' equation.
As far as the R-square values are concerned, they are all equal or above 0.94 except in two cases.

Nano-herbicide transport

The transport parameters for the nano-formulation injected in saturated columns, estimated using MNMs are summarized in Table 4. The parameters are calculated in the software by solving equation 1, and equations 14, 15, 16, and 18. The model curves fitted to the experimental data of each test are shown in Part C of the Appendix. Test 'NaCl 2' is the only test that shows a R-square value lower than 0.95, due to the high variability of the experimental values.

Table 4: estimated parameters through MNMs from tests performed with the formulation without coating.

Formulation no coating								
Test name	Type of transport	R^2 [-]	Attachment rate, $k_{a,1}$ [1/s]	Detachment rate, $k_{d,1}$ [1/s]	Ripening multiplier A [-]	Ripening exponent β [-]	s_{max} [-]	Attachment rate, $k_{a,2}$ [1/s]
NaCl 1	Ripening & linear	0.95	$2.10\text{x}10^{-03}$	$2.96\text{x}10^{-05}$	104.66	0.4901	-	$7.20\text{x}10^{-03}$
NaCl 2	Ripening & linear	0.84	$8.40\text{x}10^{-03}$	$2.92\text{x}10^{-05}$	118.02	0.7317	-	$1.5\text{x}10^{-03}$
Tap 1	Ripening & linear	0.97	$3.40\text{x}10^{-03}$	$2.40\text{x}10^{-06}$	758.46	0.8798	-	$3.60\text{x}10^{-03}$
NaCl mod pH 2	Blocking & linear	0.99	$5.10\text{x}10^{-03}$	-	-	-	$8.23\text{x}10^{-05}$	$3.20\text{x}10^{-03}$

Concerning the formulation without coating, in Figure 13 it can be seen that, when the formulation is flushed in tap water, the peak concentration values are higher than the case of the NaCl prepared formulation. This means that, when tap water is used, less particles interact with the porous medium and with each other, as the ionic strength is lower, repulsion with both porous medium and among particles is more pronounced, and therefore more particles reach the outlet. Concerning the transport parameters, this is translated into higher ripening multiplier and exponent values.

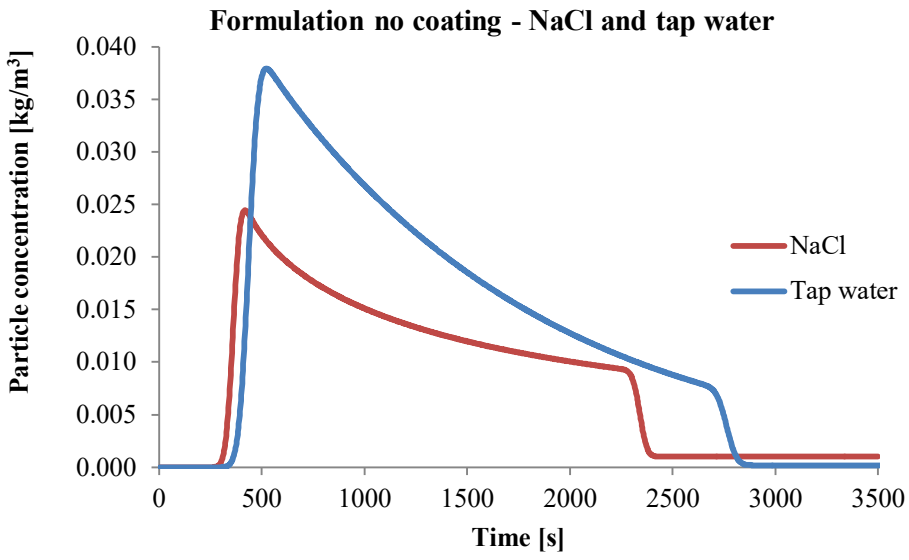

Figure 13: fitted curves in MNMs of the test in tap water and in NaCl (tests 'Tap 1' and 'NaCl 1') of the formulation with no coating.

For the formulation with no coating, ripening is observed in all tests, but one. This is the one performed at modified pH (Figure 14), which has a completely different trend and has higher concentration values of the breakthrough curve than the other cases without coating.

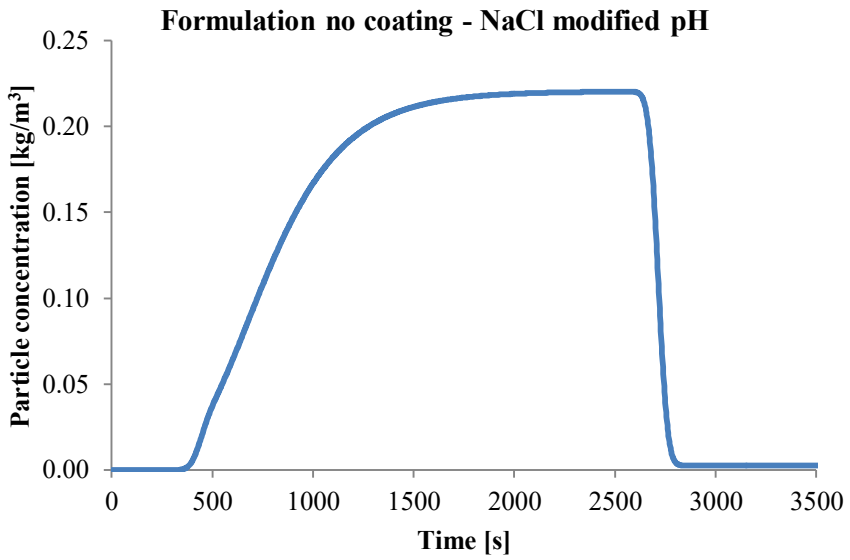

Figure 14: fitted curves in MNMs of the test in NaCl with modified pH of the formulation with no coating.

When the formulation with coating is used, a linear irreversible behavior and blocking is observed in all tests conditions (Figure 15 is shown as an example) and the peak concentration values are around the same for NaCl and tap water. Nevertheless in test 'Tap 2' the estimated curve does not totally match the experimental data.

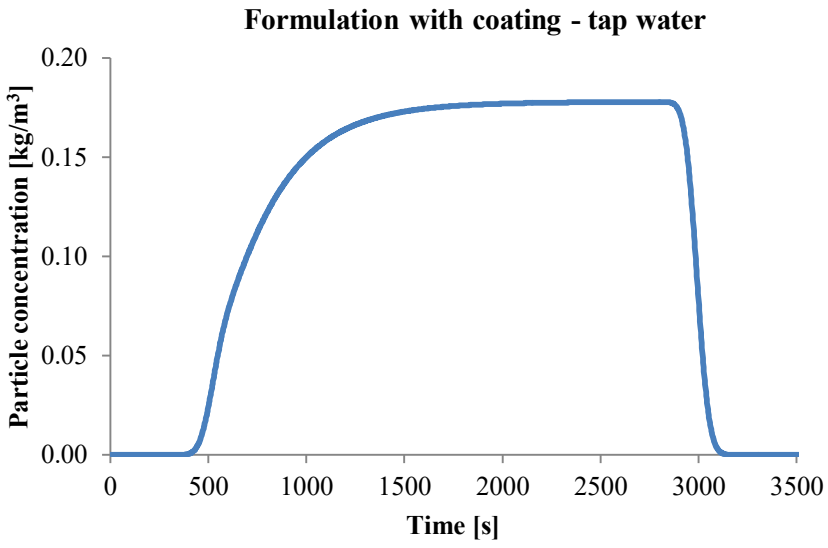

Figure 15: fitted curve in MNMs of the test in tap water of the formulation with coating.

Contrary to the case of the nano-formulation without coating, the concentration values of the test with tap water are around the same of the test using NaCl in the presence of coating. Also from the curves it can be seen that with a modified pH (Figure 16) the concentration values are higher than in the case of NaCl and water, meaning that transport is favored at slightly alkaline pH.

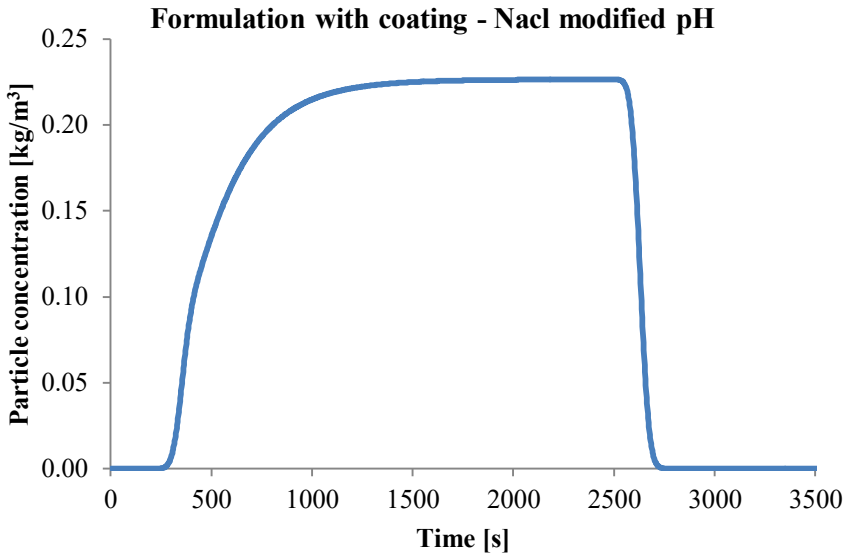

Figure 16: : fitted curve in MNMs of the test in NaCl at modified pH, of the formulation with coating.

Although the estimated parameters have the same order of magnitude in all cases, the coefficients values differ more between the test with the formulation using NaCl and the other two cases. In particular, the S_{max} value is higher with the use of water and with NaCl at modified (slightly alkaline) pH. S_{max} represents the maximum amount of particles that can be retained on the porous medium, and governs the steepness of the first part of the fitting curve, a higher value means a less steep curve and a more gradual increase of particles concentration.

Table 5: estimated parameters through MNMs from test performed with the formulation with coating.

Formulation with coating					
Test name	Type of transport	R^2	Attachment rate, $k_{a,1}$ [1/s]	s_{max} [-]	Attachment rate, $k_{a,2}$ [1/s]
NaCl 3	Linear & blocking	0.99	1.80×10^{-03}	1.40×10^{-05}	4.40×10^{-03}
NaCl 4	Linear & blocking	0.98	1.80×10^{-03}	1.25×10^{-05}	4.83×10^{-03}
Tap 2	Linear & blocking	0.99	2.49×10^{-03}	4.87×10^{-05}	3.15×10^{-03}
NaCl mod pH 2	Linear & blocking	0.98	3.00×10^{-03}	3.44×10^{-05}	3.90×10^{-03}

Comparing the two sets of experiments, the one without coating and the one with coating, it is possible to observe that ripening prevails for the no coating tests while blocking is the dominant mechanism in the tests with coating. In the case of no coating the breakthrough concentrations are lower than the case with coating, because uncoated particles are less stables and tend to interact more with the sand, resulting in less particles reaching the outlet. Test performed at modified pH always show higher concentration values in the breakthrough curve than in the other tests.

In Table 6, results from the simulation performed with clay particles only are shown. From this test it can be concluded that clays nano-particles interact with the porous medium with ripening mechanism and that their mobility is very limited.

Table 6: estimated parameters through MNMs from test performed with clay particles.

Clay only in NaCl					
Solution	Type of transport	R^2	Attachment rate k_a [1/s]	Ripening multiplier A [-]	Ripening exponent B [-]
NaCl	Ripening	0.97	4.60×10^{-03}	3329.6	1.3137

4.1.2 Unsaturated conditions

Tracer test

The results obtained from the unsaturated tracer test interpretation performed in Hydrus 1D are shown in Table 7. Again the tests are named after the solution involved in the experiment.

Table 7: data interpretation of the unsaturated tracer test, estimated parameters in Hydrus 1D.

Nano-herbicide	Test name	Unsaturated water content [-]	Dispersivity [m]	R^2
No coating	NaCl 1	0.19	1.55×10^{-04}	0.93
	Tap 1	0.17	5.45×10^{-04}	0.98
	Tap 2	0.12	7.50×10^{-04}	0.96
	NaCl pH mod 1	0.17	8.53×10^{-04}	0.92
With coating	NaCl 3	0.20	4.17×10^{-04}	0.92
	NaCl 4	0.17	5.59×10^{-04}	0.88
	Tap 3	0.16	5.11×10^{-04}	0.97
	Tap 4	0.21	2.04×10^{-03}	1.00
	NaCl pH mod 2	0.19	1.33×10^{-04}	0.76

The results from the first tracer test, only necessary for the calculation of the initial water content in the sand-packed column, are shown in Part C of the Appendix.

Nano-herbicide transport

As far as the nano-herbicide transport is concerned, only in some cases a significant breakthrough and a clear trend in the breakthrough curve can be seen (and data can be interpreted). The tests with very low or no breakthrough, corresponding to limited mobility of the nano-formulation in the unsaturated porous medium, are those performed in NaCl, with and without coating, and those in tap water without coating. Since there is no trend and the particles concentration is almost zero at the outlet, it means that most of the nano-formulation interacts with the collector from which they are attracted.

Table 8: type of test and detected behavior.

Formulation	Test name	Behavior
No coating	NaCl 1	No breakthrough
	Tap 1	No breakthrough
	Tap 2	No breakthrough
	NaCl pH mod 1	Not defined
With coating	NaCl 3	No breakthrough
	NaCl 4	No breakthrough
	Tap 3	Blocking and linear irreversible
	Tap 4	Blocking and linear irreversible
	NaCl pH mod 2	Blocking and linear irreversible

For tests performed in tap water with coating, the breakthrough curve is interpreted with a two-site interaction transport equation, where one site describes the linear irreversible behavior and the other the blocking effect.

Transport parameters estimated for the test that have shown a clear trend, are shown in Table 9. Those are calculated by the software Hydrus 1D, according to equations 11, and equations 15, 16, and 17. All the interpretations have a R-square value above 0.97.

Table 9: data interpretation of the unsaturated transport tests with a clear trend, transport parameters estimated in Hydrus 1D.

Site	Behavior	Transport parameters	Tap 3 with coating	Tap 4 with coating	NaCl pH mod 2 with coating
1	Linear irreversible	$k_{a,1}$ [1/s]	2.99×10^{-03}	2.16×10^{-03}	1.03×10^{-03}
2	Blocking	$k_{a,2}$ [1/s]	1.29×10^{-02}	4.04×10^{-03}	3.60×10^{-03}
		$k_{d,2}$ [1/s]	1.00×10^{-04}	6.62×10^{-05}	3.20×10^{-03}
		S_{max} [-]	1.03×10^{-07}	1.47×10^{-07}	7.45×10^{-08}

4.2 Field-scale scenario simulations

The different scenarios are described in section '3.3 Scenario simulations'.

Transport parameters from the test named 'tap 3' with coating are used as inputs to simulate the nano-herbicide formulation behavior in the 3D domain. The formulation without coating that was mainly absorbed by the collector is simulated assuming a linear irreversible behavior with a very high transport coefficient and a very low detachment coefficient. The conventional herbicide is simulated as a conservative solute with no sorption nor degradation.

In Table 10 the transport parameters used in the simulations for each of the formulation and the test from which the data is obtained are reported.

Table 10: transport parameters corresponding to each simulated nano-formulation and the corresponding column test data.

Formulation	Transport parameters [1/s]	Corresponding test
Nano-herbicide with coating	$k_{a,1} = 2.99\text{x}10^{-3}$ $k_{a,2} = 1.29\ \text{x}10^{-2}$ $k_{d,1} = 1.00\ \text{x}10^{-11}$ $k_{d,2} = 1.00\ \text{x}10^{-4}$	Tap 3 with coating
Nano-herbicide without coating	$k_a = 0.10$ $k_d = 1.00\ \text{x}10^{-11}$	Tap 1 no coating

In the following section, results from the simple cubic geometry are first shown for scenario A,B, and C then the simulation for the larger scale geometry that considers an aquifer is shown.

4.2.1 Simulations in a simple geometry

Scenario A. Injection of the formulation in regular weather conditions.

In Figure 17 the concentration profiles in the liquid phase are shown at different times: right after the herbicide has been applied and after 6 hours from the application. The trend of normalized concentration versus the depth is in accordance with the expected behavior of the formulation.

After 6 hours from the application, the conventional herbicide shows higher values at deeper depth. Conversely, the nano-formulations show a limited mobility and the herbicide nano-particles mainly remain in the upper part of the subsoil. Lower mobility is observed for the formulation without coating, coherently with the trend observed in column tests and modeled in the 1D simulations (Figure 18).

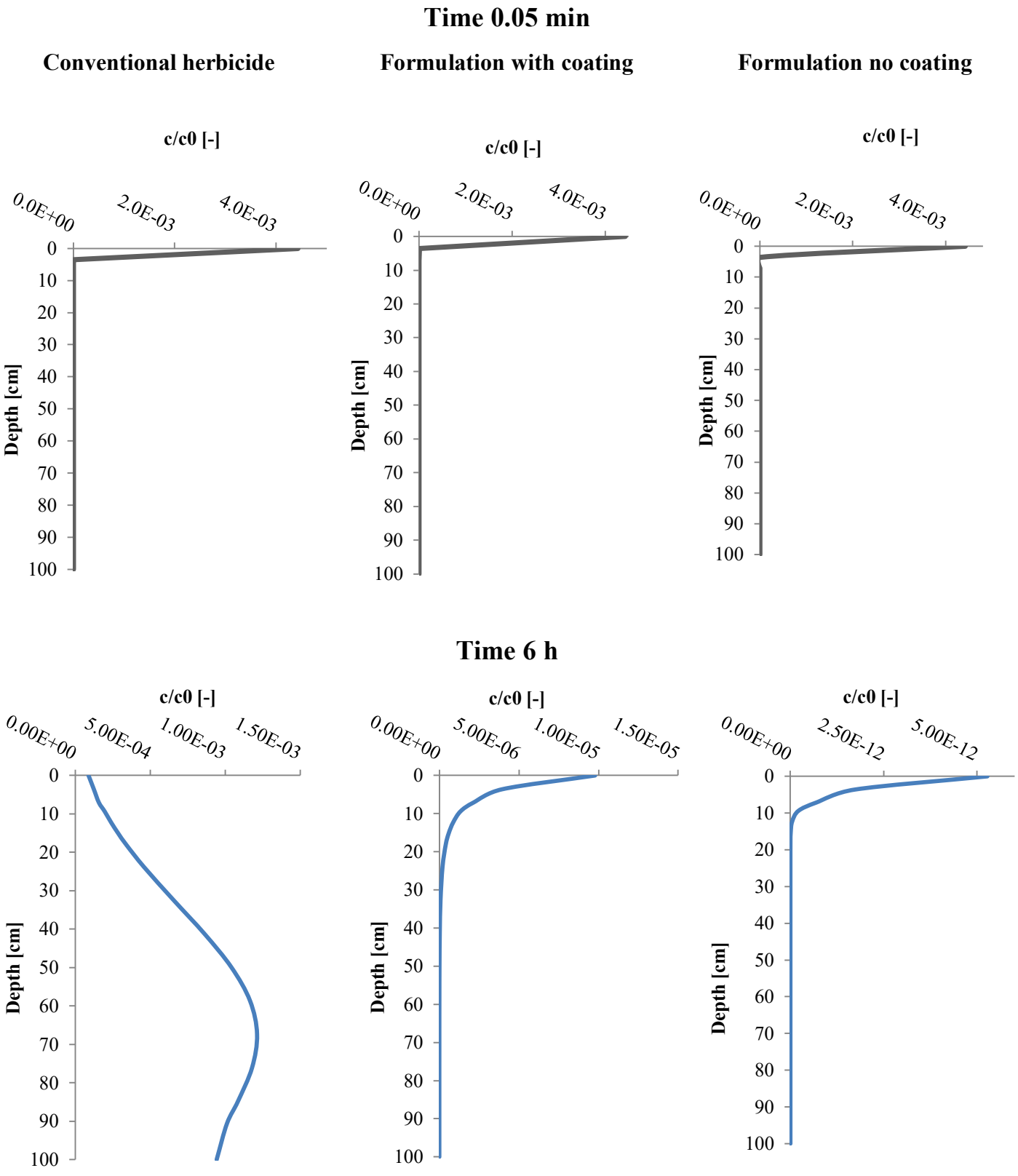

Figure 17: scenario A, normalized concentration in the liquid phase versus depth of a conventional herbicide and the two formulations at 0.05 min and at 6 hours from application, modelled in HYDRUS.

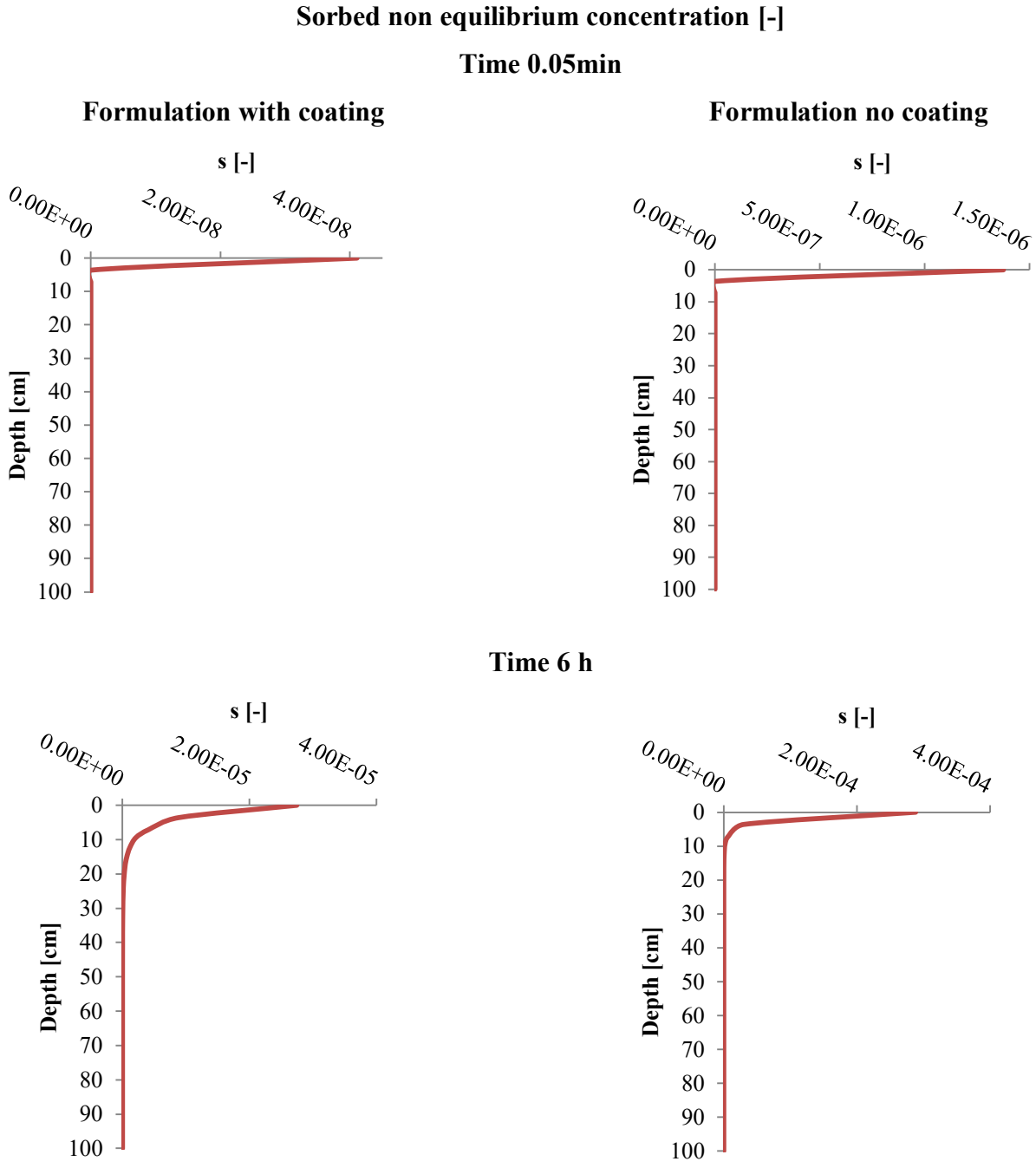

Figure 18: scenario A, concentration in the solid phase versus depth of a conventional herbicide and the two formulations at 0.05 min and at 6 hours from application, modelled in HYDRUS.

Scenario B. Injection of the formulation and 6 hours of rain.

The scenario B simulation results are observed at the beginning of the rainy event (after 1 hour), at the end of the precipitation (after 6 hours) and six hours after the precipitation is over (at 10 hours from the beginning of the simulation).

In Figure 19 results are shown for the conventional herbicide, in Figure 20 for the formulation with coating and for the one without coating with also the solid phase concentration

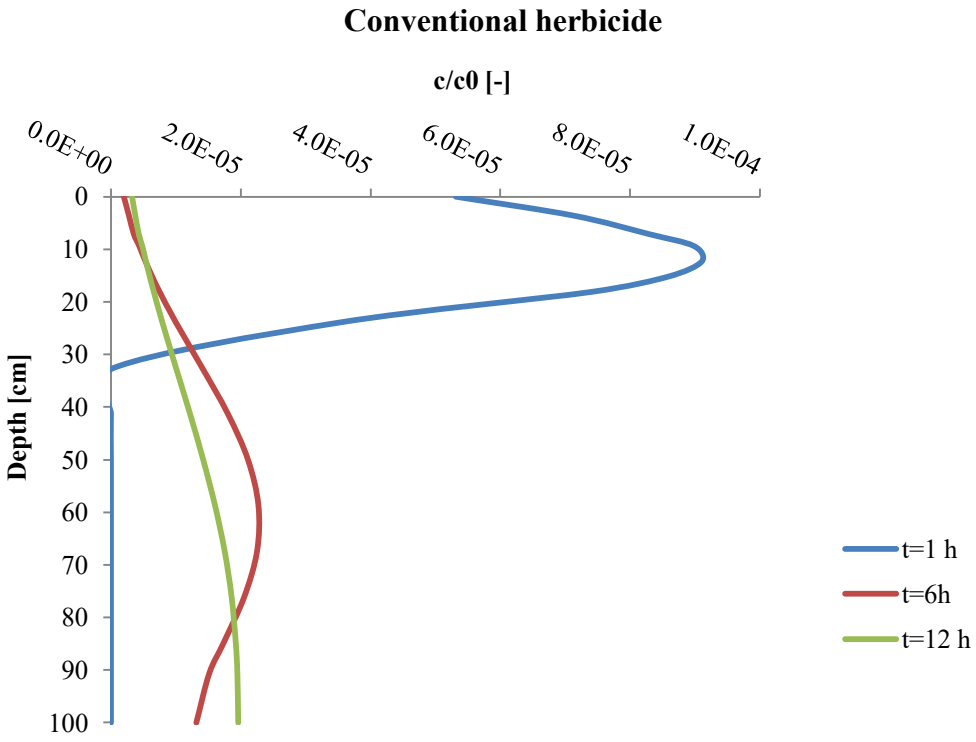

Figure 19: scenario B, concentration in the liquid phase versus depth of the conventional pesticide at different times, results from HYDRUS.

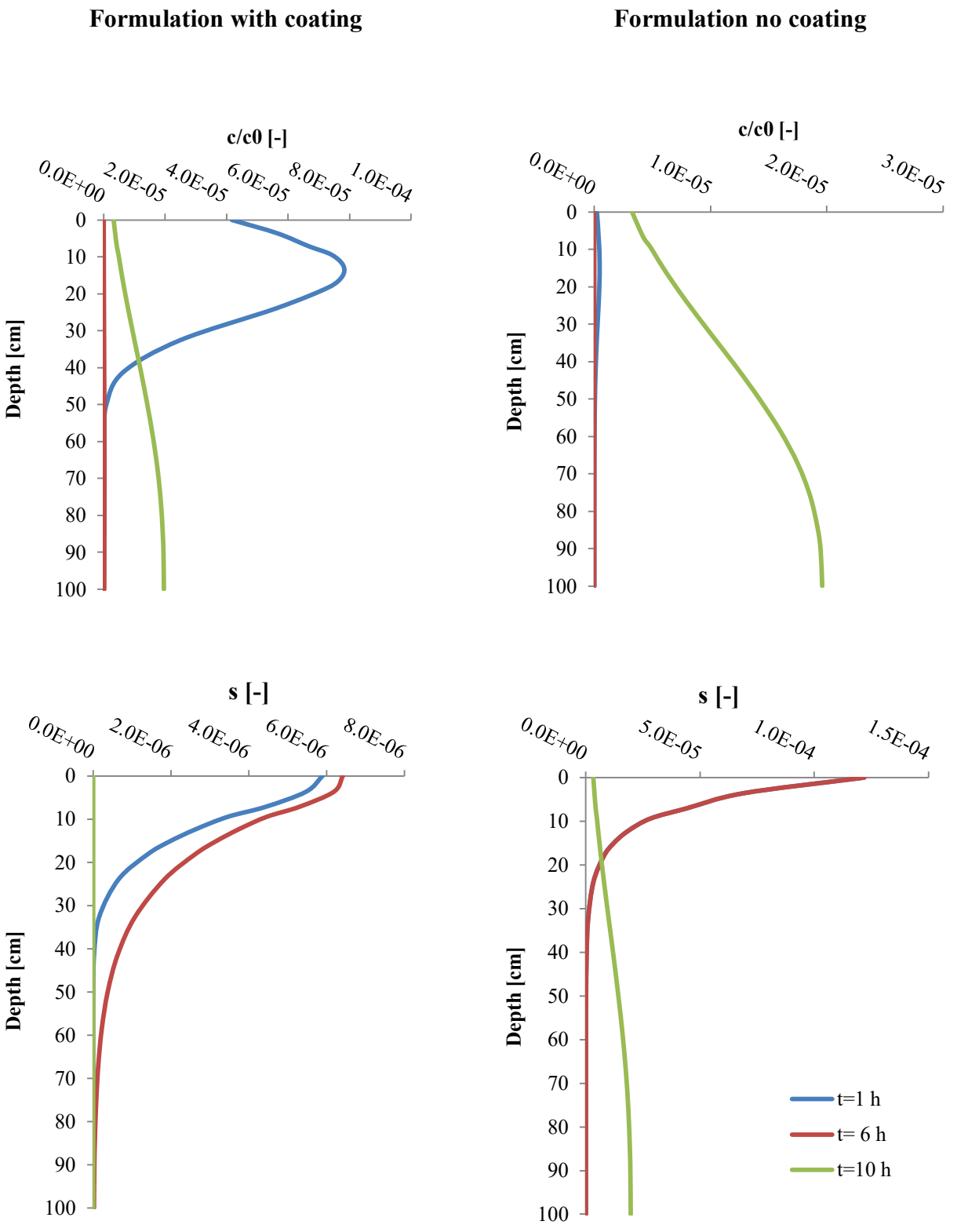

Figure 20: scenario B, concentration in the liquid phase (above) and in the solid phase (below) versus depth of the formulation with and without coating, at different times, results from HYDRUS.

When rain occurs it is possible to see that at 6h and 10h the mobility of the formulation with coating is reduced compared to the conventional one. The nano-formulation sticks to the solid phase in the first 60 cm. It is interesting to look at the behavior of the formulation with no coating which firstly present a very low concentration in the liquid phase but then at 10 h it becomes higher, as if some particles are released.

Scenario C. Injection of the formulation and irrigation.

The concentration is observed at 10 minutes, which is the time for which the pressure head boundary condition is valid, one hour and three hours. At three hours the concentrations in the liquid phase are always around 0, this means that the herbicide is transported away, but in the case of the nano-herbicide, concentration values in the liquid phase are lower and a low concentration in the solid phase can be seen at lower depth.

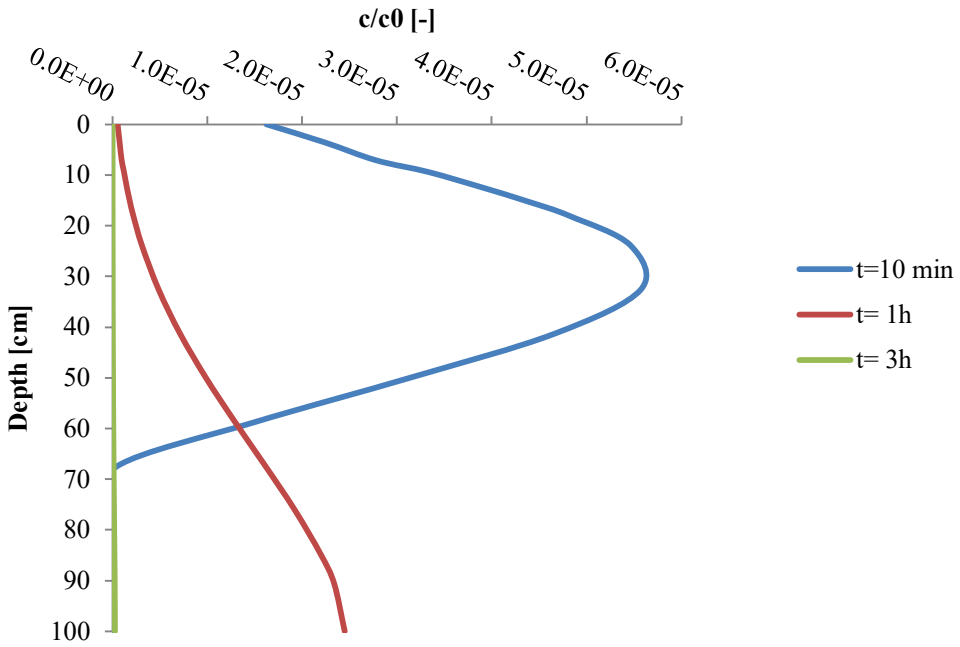

Figure 21: scenario C, normalized concentration in the liquid phase vs. depth for the conventional herbicide at different times, results from HYDRUS.

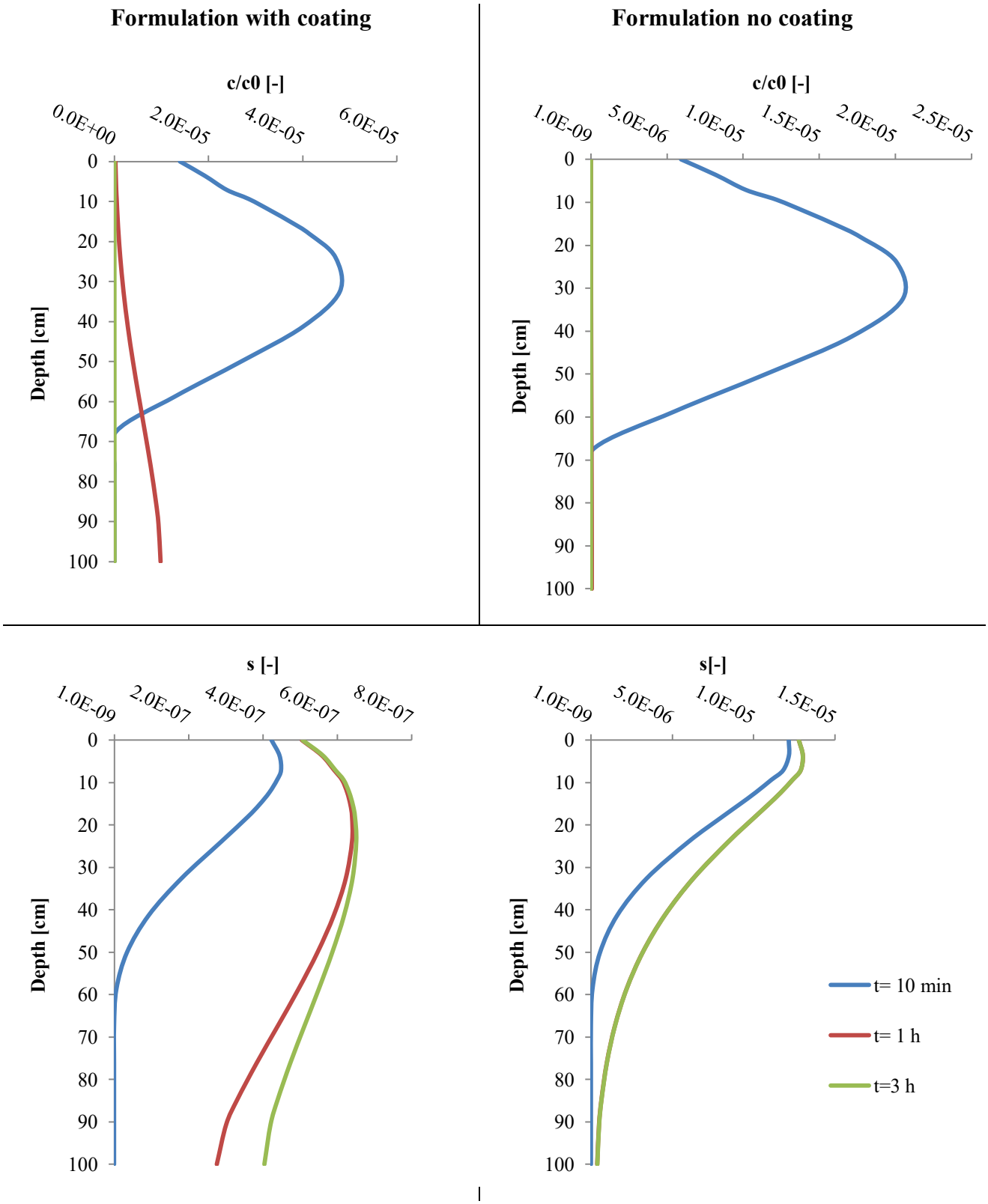

Figure 22: scenario C, concentration in the liquid phase (above) and in the solid phase (below) versus depth of the formulation with and without coating, at different times, results from Hydrus

4.2.2 Field simulation in the presence of an aquifer

Considering the second geometry, from the results of the B scenario simulations (herbicide application and heavy rain), it can be seen that both the herbicide and the nano-herbicide, spread along the vertical direction in the vadose zone, due to the effect of rain. Lateral spreading at the surface is limited.

When the simulation is run for a conventional herbicide, the formulation reaches the aquifer and then the concentration gradually increases and the herbicide begins to move in the flow direction (Figure 23). After 7 days, which includes 6 hours of heavy rain, the herbicide has been transported for around 8 meters in the aquifer.

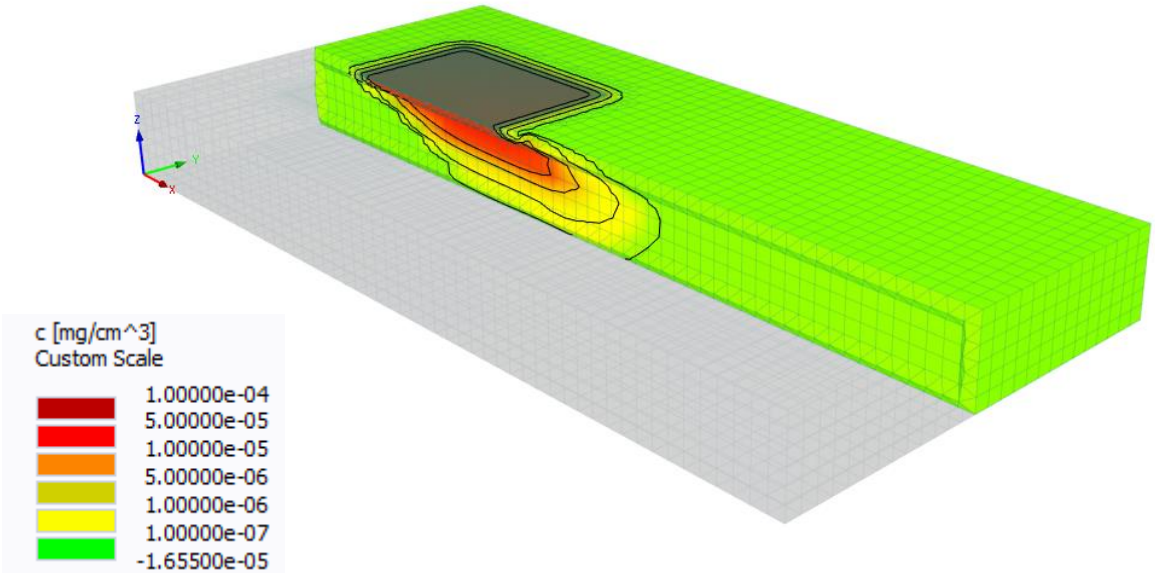

Figure 23: scenario B. Conventional herbicide concentration in the subsoil at 7 days from application, simulation in HYDRUS.

The nano-herbicide, modelled with the transport parameters of the 'Tap 3' test with coating, is not very mobile. A concentration over 1 x 10^{-7} mg/cm^3, is never seen on the aquifer during the time frame considered. The lowest concentration value is seen 80 cm below the surface after 2 hours of rain. A clear dispersion in the aquifer is not seen (Figure 24), because the herbicide mostly stays in the first centimeters of depth. The sorbed concentration is seen only up to 10 cm with very low concentrations (Figure 25).

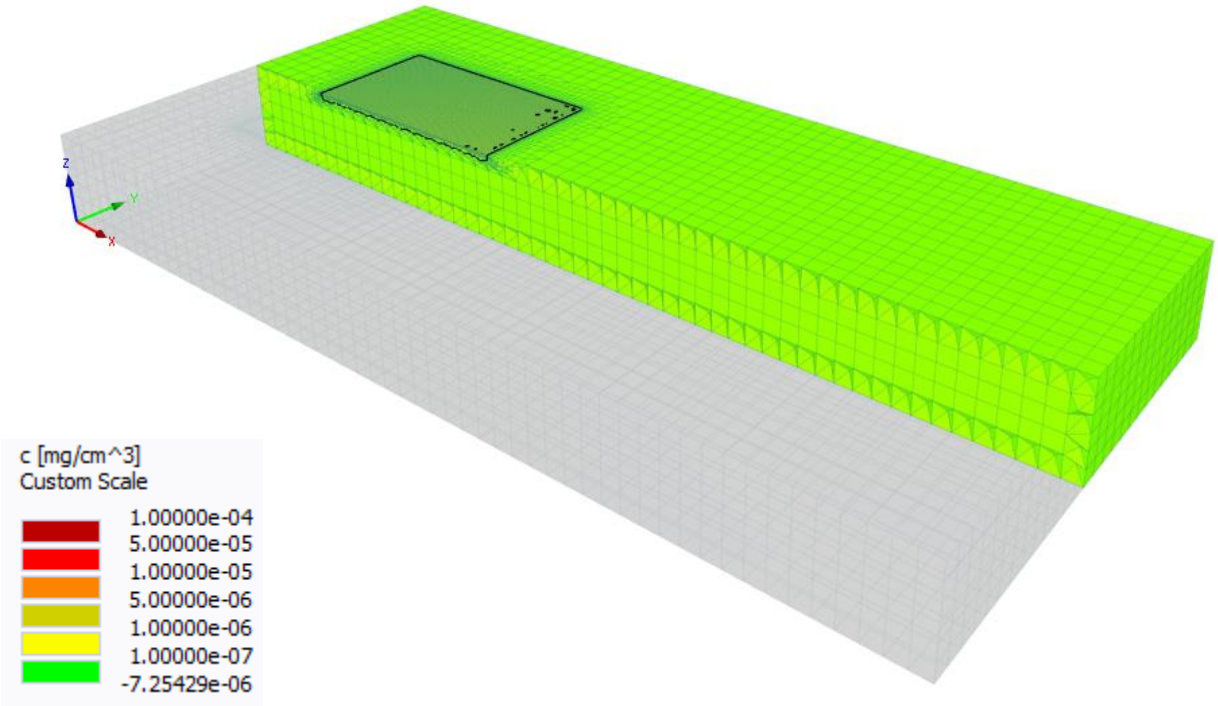

Figure 24: scenario B. Nano-herbicide concentration in the subsoil at 7 days from application, simulation in HYDRUS.

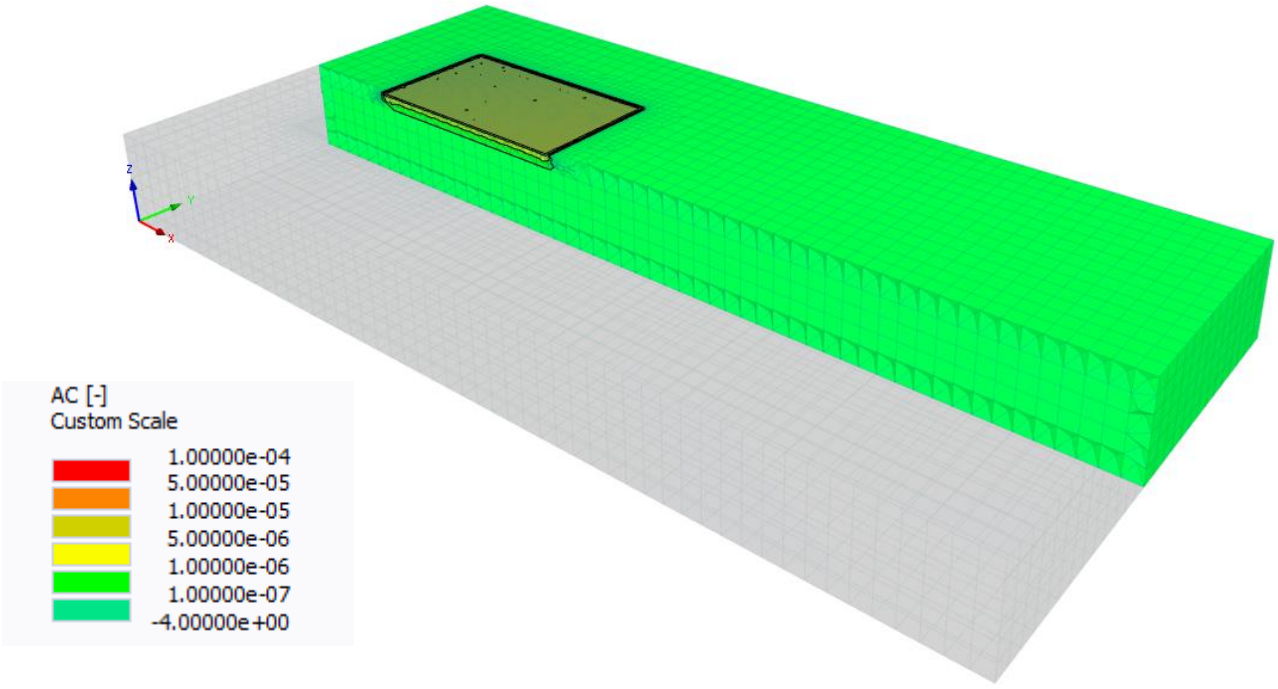

Figure 25: scenario B. Nano-herbicide sorbed concentration in the subsoil at 7 days from application, simulation in HYDRUS.

The formulation without coating is even less mobile and stays even more in the upper layers of the subsoil than the one with coating. For the purpose of evaluating a potential infiltration in the aquifer, there was no reason of modelling it in this geometry as no more conclusions would have been drawn.

These results inherit uncertainties, because several assumptions have been made when building the model, such as no degradation is considered and no volatilization. Nevertheless they clearly show that the nano-formulation has a lower mobility in the liquid phase compared to the use of a traditional herbicide. In particular it moves but with much lower concentration than a conventional herbicide and mainly stays in the upper part of the vadose zone. These models can be useful to predict the dispersion of the herbicide in the subsoil and study what happens to the environmental fate of the formulation after it is applied on field, but they are also useful as a tool for future risk assessments.

5. Conclusions

The data interpretation has shown that, in saturated conditions, the use of NaCl or tap water does not affect much the behavior of the injected particles. However the behavior changes when coating is applied to the nano-herbicide. Different results are obtained for the unsaturated tests. In unsaturated conditions in many cases (when using NaCl solution with and without coating and when using tap water for the formulation without coating) no significant breakthrough of the nano-formulation is observed because most of the nano-herbicide sticks to the porous material inside the column. A clear breakthrough curve is observed only when tap water and NaCl at modified pH are used when the formulation has a coating.

The behavior of the two different nano-formulations, with and without coating in tap water, has been modelled in a field-like synthetic scenario and compared to the behavior of a traditional herbicide. In the three dimensional modelling in HYDRUS, different scenarios have been considered: a regular application in good weather conditions, an application followed by heavy rain for 6 hours, an application followed by irrigation. The field-scale scenario modelling shows that in all considered scenarios, the nano-formulation compared to a traditional herbicide is less mobile.

The nano-herbicide concentrations in the liquid phase at field scale are always lower than the traditional herbicide, meaning that the possibility for the active ingredient to be transported in water and to potentially reach aquifers or water bodies increasing the risk of pollution, only involves a restricted amount of the active ingredient. When using the nano-formulation an amount of herbicide remains attached to the first decimeters of the vadose zone. This property could potentially enhance the target application of the herbicide, restraining it to the upper part of the subsoil.

The simulation of the field-like scenarios can be a first step in the development of a multi-scale approach in support of fate studies, combining laboratory data and modeling. When modelling, many simplifying assumptions are made, however the performed simulations could be very useful to predict the transport of the herbicide in the subsoil at different conditions. A calibrated and validated model with data collected on field is the next step for a more real-like scenario and to draw more realistic conclusions. Also, more scenarios should be considered in order to study

thoroughly the mobility of the nano-formulation at different conditions, that take into account highly variable weather conditions for example.

The built model could also be used as input for new risk assessment evaluations of the nano-formulation. Nowadays risk assessments methods, that consider pesticides as solutes, are standardized and widely used. The introduction of nano-pesticides has now questioned the validity of traditional assessment methods, because they may exclude relevant characteristics of nano-pesticides. A new ad hoc regulatory framework for nano-pesticides is required.

To conclude, the nano-herbicide is very promising and fulfill the first hypothesis. The data interpretation and modelling phase have shown that the herbicide is less mobile. The use of the nano-herbicide solves two of the drawbacks related to herbicides use. Firstly, because of the formulation (combination of active ingredient with clay nano-particles), a lower amount of active ingredient is needed during application, overcoming the problem of conventional herbicide overdose and losses during application. Secondly and most importantly, because of the reduced mobility, it lowers the risk of the active ingredient uncontrolled transport and potential sites pollution in the subsoil and near water bodies.

Further studies, a new regulatory framework, tests, and research needs to be performed before drawing any further conclusion, but at this stage it can be said that the nano-formulation could be a promising solution because it has a reduced mobility and it reduced the uncontrolled dispersion of the herbicide in the subsoil.

Bibliography

Adamczyk, Z., Siwek, B., Zembala, M. & Belouschek, P., 1994. Kinetics of localized adsorption of colloid particles. *Advances in Colloid and Interface Science,* Volume 48, pp. 151-280.

Arpa Piemonte, 2019. *Meteo - Intensità precipitazione.* [Online]
Available at:
https://www.arpa.piemonte.it/rischinaturali/tematismi/meteo/osservazioni/radar/intensita-precipitazione.html?delta=0
[Accessed 01 September 2019].

Balaure, P., Gudovan, D. & Gudovan, I., 2017. Nanopesticides: a new paradigm in crop protection. *New Pesticides and Soil Sensors,* pp. 129-192.

Bianco, C., Tosco, T. & Sethi, R., 2018. *A comprehensive tool for design and interpretation of colloidal particle transport in 1D Cartesian and 1D radial systems.,* Torino: Politecnico di Torino.

Di Molfetta, A. & Sethi, R., 2012. *Ingegneria degli acquiferi.* Milano: Springer.

EFSA, 2018. *European Food and Safety Authority. How Europe ensures pesticides are safe.* [Online]
Available at: http://www.efsa.europa.eu/en/interactive-pages/pesticides-authorisation/PesticidesAuthorisation#pesticides
[Accessed August 10 2019].

Elimelech, M., Gregory, J., Jia, X. & Williams, R. A., 1995. *Particle Deposition and Aggregation, Measurement, Modelling, and Simulation.* USA: Butterworth Heinemann.

Elimelech, M. & O'Mella, C. R., 1990. Kinetics of Deposition of Colloidal Particles in Porous Media. *Environmental Science & Technology,* Volume 24, pp. 1528-1536.

European Commission, 2012. *Pesticides.* [Online]
Available at: https://ec.europa.eu/food/plant/pesticides_en
[Accessed 10 August 2019].

European Commission, 2016. *EU - Pesticides database.* [Online]
Available at: https://ec.europa.eu/food/plant/pesticides/eu-pesticides-database/public/?event=homepage&language=EN
[Accessed 10 August 2019].

European Parliament and Council, 2009. *EUR-Lex.* [Online]
Available at: https://eur-lex.europa.eu/legal-content/EN/ALL/?uri=CELEX:02009L0128-20091125
[Accessed 10 August 2019].

Granetto, M., 2018. *A novel herbicide formulation to reduce the environmental impact of agrochemicals.* [Online]
Available at:
https://webthesis.biblio.polito.it/view/creators/Granetto=3AMonica=3A=3A.default.html
[Accessed 12 June 2019].

GW@POLITO, 2014. *MNMs 2018.* [Online]
Available at: https://areeweb.polito.it/ricerca/groundwater/software/mnms/
[Accessed 15 March 2019].

IUPAC, 1997. *International Union of Pure and Applied Chemistry. Compendium of Chemical Terminology, 2nd ed. (the "Gold Book"). Compiled by A. D. Mc-Naught and A. Wilkinson.* 2nd ed. Oxford, UK: Blackwell Scientific Publications.

Kah, M. & Hofmann, T., 2014. Nanopesticide research: current trends and future priorities. *Environment International,* Volume 63, pp. 224-235.

Kah, M., Kookana, R. S., Gogos, A. & Bucheli, T. D., 2018. A critical evaluation of nanopesticides and nanofertilizers against their conventional analogues. *Nature Nanotechnology,* Volume 13, pp. 677-684.

Kretzschmar, R., Borkovec, M., Grolimund, D. & Elimelech, M., 1999. Mobile subsurface colloids and their role in contaminant transport. *Advances in Agronomy,* Volume 66, pp. 121-193.

Logan, B. E. et al., 1995. Clarification of clean-bed filtration models. *Journal of Environmental Engineering,* Volume 121, pp. 869-873.

Mualem, Y., 1976. A new model for predicting the hydraulic conductivity of unsaturated porous media. *Water Resources Research,* 13(3), pp. 513-522.

Osman, K. & Abdulrahman, H., 2003. Risk assessment of pesticide to human and the environment. *Saudi Journal of Biological Science,* Volume 10, pp. 81-106.

Ouyang, Y., Shinde, D., Mansell, R. S. & Harris, W., 1996. Colloid-enhanced transport of chemicals in subsurface environments: a review. *Critical Reviews in Environmental Science and Technology,* 26(2), pp. 189-204.

Popp, J., Pető, K. & Nagy, J., 2013. Pesticide productivity and food security. A review. *Agronomy for Sustainable Development,* 33(1), pp. 243-255.

Re, 2019. *Dispersione in ambiente di prodotti fitosanitari (unpublished master's thesis).* Turin, Italy: Politecnico di Torino.

Richards, L. A., 1931. Capillary conduction of fluid through porous mediums. *Physics,* Volume 1, pp. 318-333.

Šimůnek, J. et al., 2013. *The HYDRUS-1D Software Package for Simulating the One-Dimensional Movement of Water, Heat, and Multiple Solutes in Variably-Saturated Media,* Riverside, California: Department Of Environmental Sciences.

Šimůnek, J. et al., 2013. *The HYDRUS-1D Software Package for Simulating the One-Dimensional Movement of Water, Heat, and Multiple Solutes in Variably-Saturated Media. Version 4.17.* Riverside, California: Department of Environmental Sciences.

Simunek, J., Sejna, M. & van Genuchten, M., 2019. *PC-PROGRESS Engineering software developer.* [Online]
Available at: https://www.pc-progress.com/en/Default.aspx?hydrus-1d
[Accessed 15 June 2019].

Šimůnek, J., Šejna, M. & van Genuchten, M. T., 2012. The C-Ride Module for HYDRUS (2D/3D) Simulating Two-Dimensional Colloid-Facilitated Solute Transport in Variably-Saturated Porous Media. Version 1.0. *PC Progress.*

Souza, L. R. R., da Rocha Neto, A. C., Franchi, L. P. & de Souza, T. A. J., 2019. Green Synthesis Approaches of Nanoagroparticles. In: *Nanobiotechnology in Bioformulations.* s.l.:Springer, pp. 353-380.

Tosco, T., 2017. *Nanotechnologies for green herbicides.* [Online]
Available at:
http://www.researchers.polito.it/en/success_stories/metti_in_rete_projects/nanotechnologies_for_green_herbicides
[Accessed 5 July 2019].

Tosco, T., Bianco, C. & Sethi, R., 2018. *A comprehensive tool for design and interpretation of colloidal particle transport in 1D Cartesian and 1D radial systems-TUTORIAL,* Torino: Politecnico di Torino.

Tosco, T. & Sethi, R., 2009. MNM1D: A numerical code for colloid transport in porous media: Implementation and validation.. *American Journal of Environmental Sciences,* Volume 5(4), pp. 516-524.

Tosco, T. & Sethi, R., 2010. Transport of non-newtonian suspensions of highly concentrated micro- and nanoscale iron particles in porous media: A modeling approach. *Environmental Science and Technology,* 44(23), pp. 9062-9068.

United Nations, 2015. *Sustainable Development Goals.* [Online]
Available at: https://sustainabledevelopment.un.org/
[Accessed 10 August 2019].

United Nations, 2019. *World Population Prospects 2019: Highlights,* Department of Economic and Social Affairs: Population Division.

van Genuchten, M. T., 1980. A Closed-form Equation for Predicting the Hydraulic Conductivity of Unsaturated Soils. *Soil Science Society of America Journal,* Volume 44, pp. 892-898.

van Genuchten, M. T., Leij, F. J. & Yates, S. R., 1991. *The RETC Code for Quantifying the Hydraulic Functions.* EPA/600/2 - 91/065 ed. Washington DC: United Stated Environmental Protection Agency.

van Genuchten, M. T. & Pechepsky, Y., 2011. Hydraulic Properties of Unsaturated Soils. In: *Encyclopedia of Agrophysics.* s.l.:Springer, pp. 368-376.

Worrall, E. et al., 2018. Nanotechnology for plant disease management. *Agronomy,* 8(285).

Appendix

Part A

Single collector efficiency

The transport step, the phase where the particles are carried closer to the surface of the porous medium is described by the single collector contact efficiency. This phase is governed by:

- particles interception of grains of the porous medium,
- gravitational sedimentation, due to sedimentation of particles when the density of them is higher than water,
- Brownian diffusion caused by Brownian thermal movement.

The single-collector efficiency η [-] is calculated as the sum of the terms representing the removal by each of the three different mechanisms:

$$\eta = \eta_D + \eta_I + \eta_S \tag{22}$$

The term η_D is the one accounting for diffusion, and is defined as:

$$\eta_D = 4{A_s}^{1/3} N_{Pe}^{-2/3} \tag{23}$$

where:

- A_s is a correction factor [-], defined as:

$$A_s = \frac{2(1-\gamma^5)}{2-3\gamma+3\gamma^5-2\gamma^6} \tag{24}$$

with:

$$\gamma = (1-\theta)^{1/3} \tag{25}$$

- N_{Pe} is the Peclet number [-], given by:

$$N_{Pe} = \frac{3\pi\mu d_p d_c q}{kT} \tag{26}$$

in which:

- μ is the fluid viscosity, $\mu = 0.00093$ Pa s [$ML^{-1}T^{-1}$],
- d_p is the diameter of the colloidal particles [L],
- q is the Darcy's flux [LT^{-1}],
- k is the Boltzman constant, $k = 1.38048 \times 10^{-23}$ J/K [$M\,L^2T^{-2}K^{-1}$],
- T is the temperature, $T = 298$ K [K].

The term accounting for interception, η_I, is defined as:

$$\eta_I = A_s N_{Lo}^{1/8} N_R^{15/8} \tag{27}$$

where the parameters that have not been previously defined are:

- N_{Lo} [-] that accounts for the contribution of particle London-van der Walls attractive forces to particle removal:

$$N_{Lo} = \frac{4H}{9\pi\mu d_p^2 q} \tag{28}$$

where, besides the terms previously defined:

- H is the Hamaker constant, $H = 1\text{e}-20$ J, [ML^2T^{-2}]

The term taking into account for gravitational sedimentation, η_S, is defined as:

$$\eta_S = 0.00338 A_s N_G^{1.2} N_R^{-0.4} \quad (29)$$

where:

- N_G is the gravitation number defined as:

$$N_G = \frac{g(\rho_p - \rho_f) d_p^2}{18 \mu q} \quad (30)$$

where:

- g is the gravitational acceleration, $g = 9.81$ ms^{-2} [LT^{-2}],
- ρ_p is the bacterial density $\rho_p = 1080$ kgm^{-3} [ML^{-3}],
- ρ_f is the fluid density $\rho_f = 998$ kg m^{-3} [ML^{-3}]

Colloidal particles interactions

Colloidal particles can attract each other and can deposit onto the solid matrix. These kind of interactions have an important role at short distance, as they affect the transport of colloids in the porous medium (Elimelech & O'Mella, 1990). The interaction behavior can be defined by the Derjaguin-Landau-Verwey-Overbeek theory, DLVO theory, which describes the total involved interaction energy, taking into account the van der Waals attraction forces and the electric double layers repulsive forces.

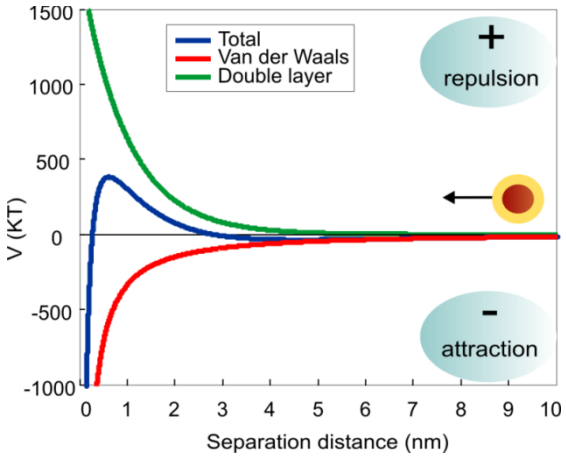

Figure 26: particle-collector interaction energy. Source: course slides of Prof. Tosco.

Considering the Van der Waals attraction and the electrical double layer repulsion the interaction between particles and between particles and collector can be (Figure 27):

- completely repulsive
- completely attractive
- repulsive and attractive, based on the distance between the surfaces involved.

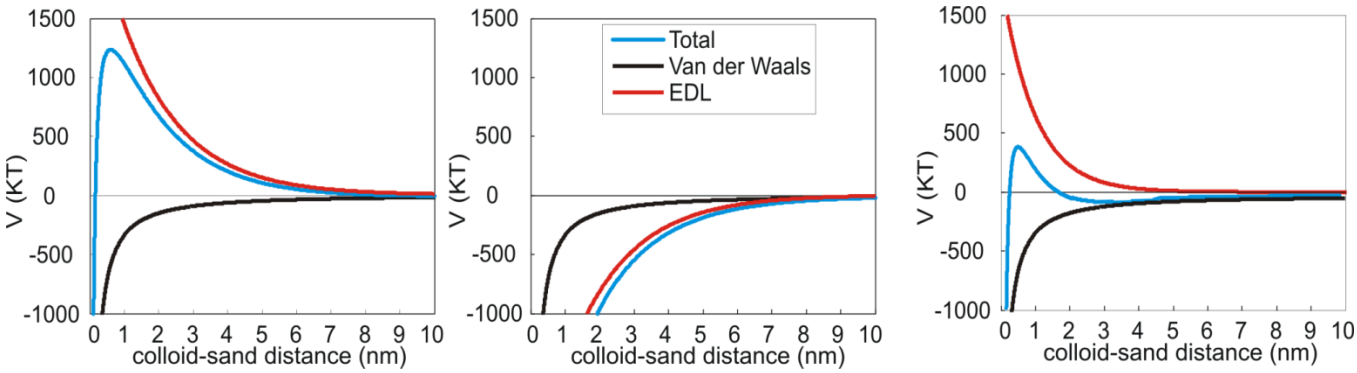

Figure 27: interaction profiles of colloid-collector. Left: repulsive profile, center: attractive profile, right: repulsive and attractive. Source: course slides of Prof. Tosco.

The DLVO theory however is insufficient to take into account all the possible interactions. Therefore the following interactions were added to the classical DLVO theory:

- Born repulsion
- Steric interaction
- Magnetic interaction

Knowledge of the particles interaction is important to understand their behavior and transport in the saturated porous medium.

Part B

Observation points (Table 11) set in the simple cubic geometry, with the same x and y coordinates at the middle of the cube.

Table 11: depths of the added observation points.

Observation point	Depth [cm]
1	0.00
2	3.60
3	7.10
4	9.40
5	12.30
6	15.20
7	18.10
8	23.90
9	32.60
10	41.30
11	50.00
12	58.70
13	67.40
14	76.10
15	84.80
16	90.60
17	100.00

Part C

Nano-herbicide transport in saturated conditions

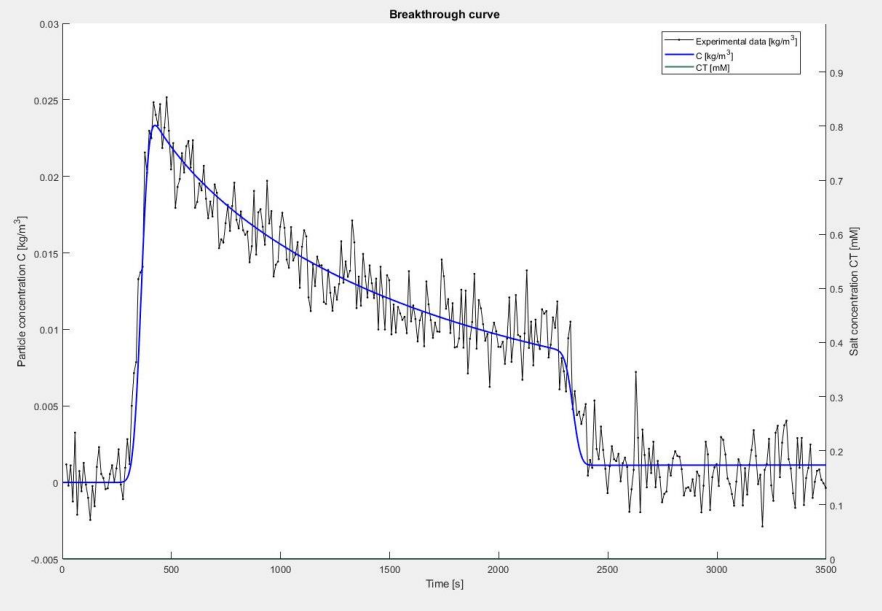

Figure 28: test 'NaCl 1', transport simulation in MNMs of the formulation without coating prepared in NaCl.

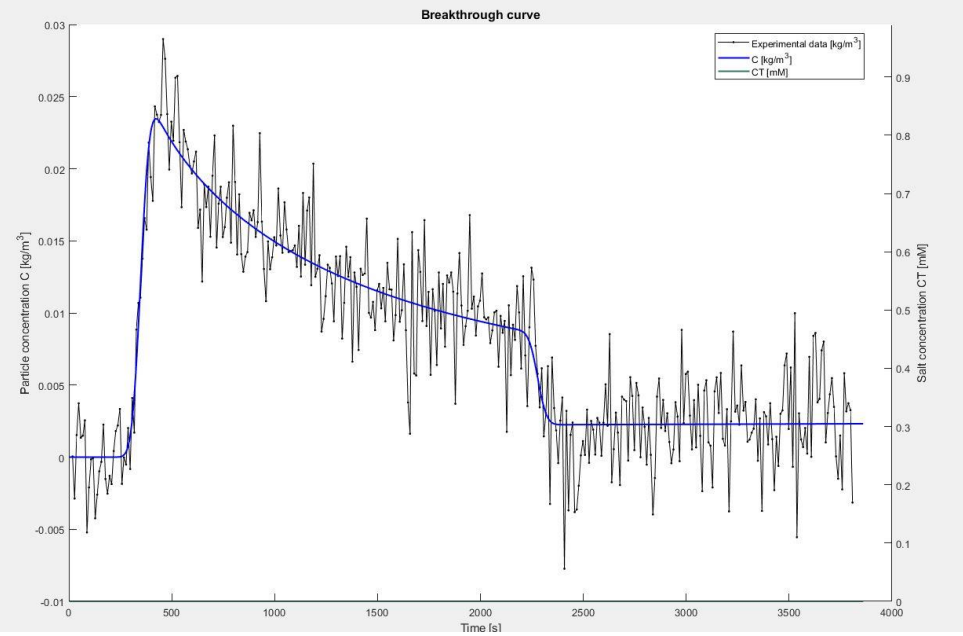

Figure 29: test 'NaCl 2', transport simulation in MNMs of the formulation without coating prepared in NaCl.

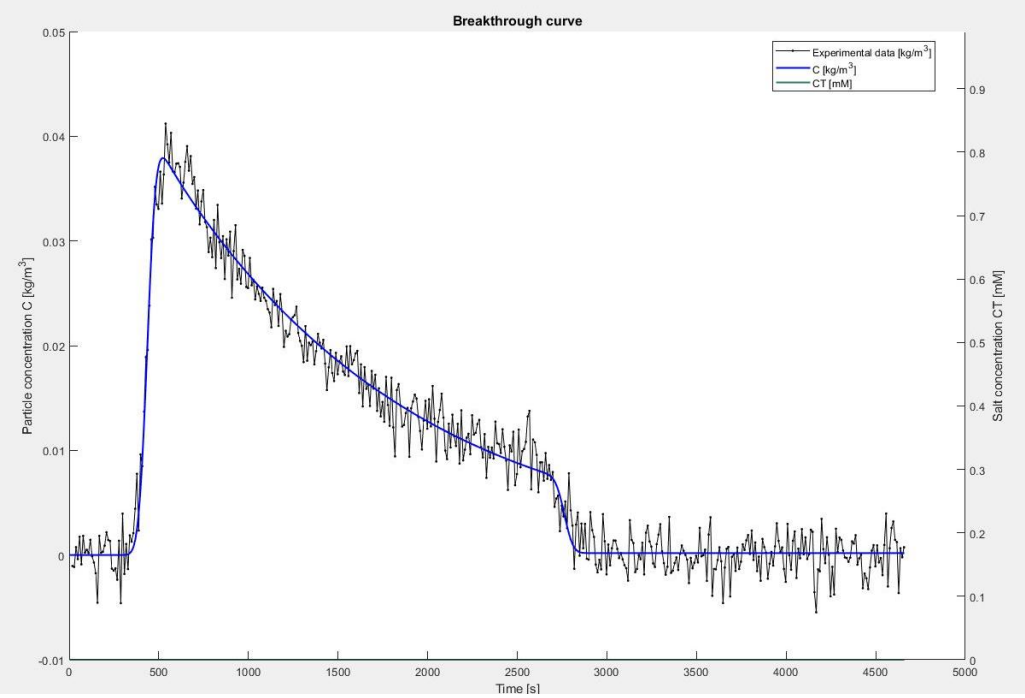

Figure 30: test 'Tap 1', transport simulation in MNMs of the formulation without coating prepared in tap water.

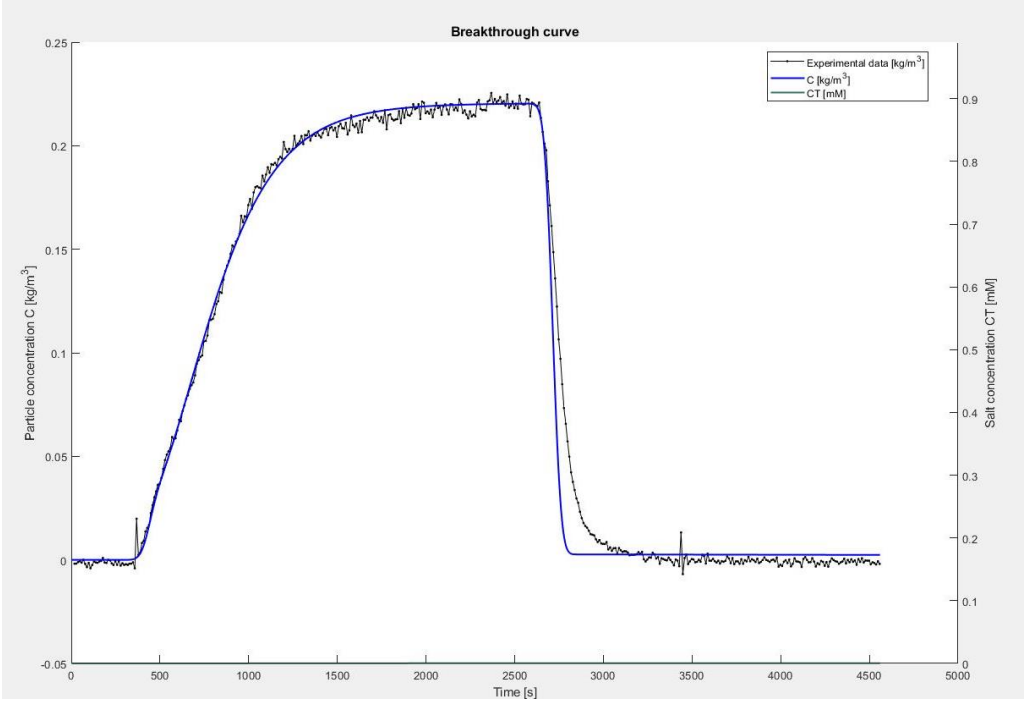

Figure 31: test 'NaCl mod Ph 1', transport simulation in MNMs of the formulation without coating prepared in NaCl with modified pH.

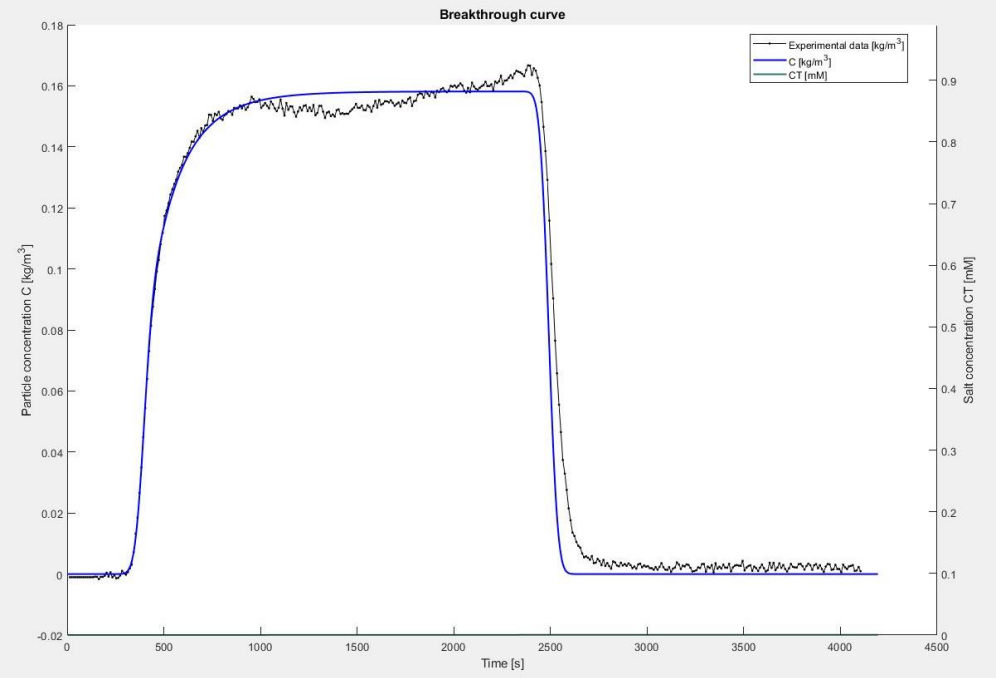

Figure 32: test 'NaCl 3' transport simulation in MNMs of the formulation with coating prepared in NaCl.

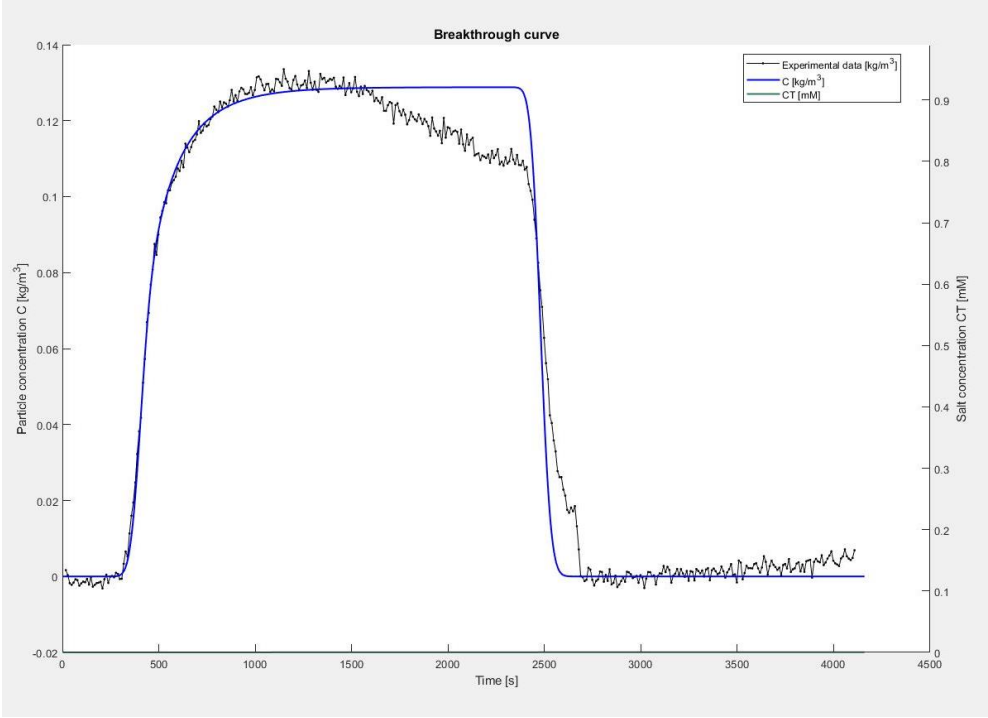

Figure 33: test 'NaCl 4', transport simulation in MNMs of the formulation with coating prepared in NaCl.

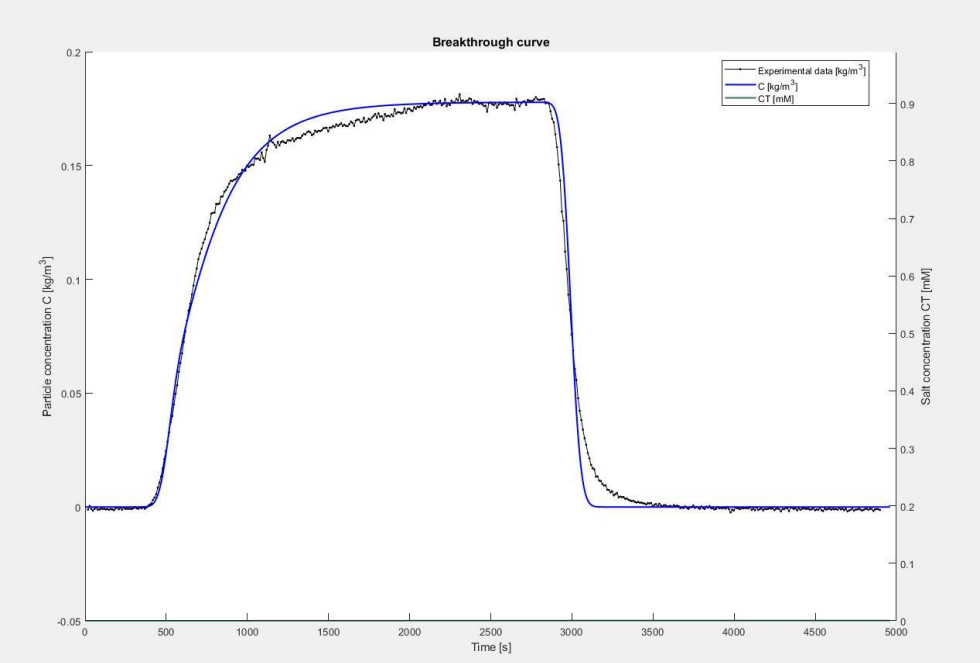

Figure 34: test 'Tap 2', transport simulation in MNMs of the formulation with coating prepared in tap water.

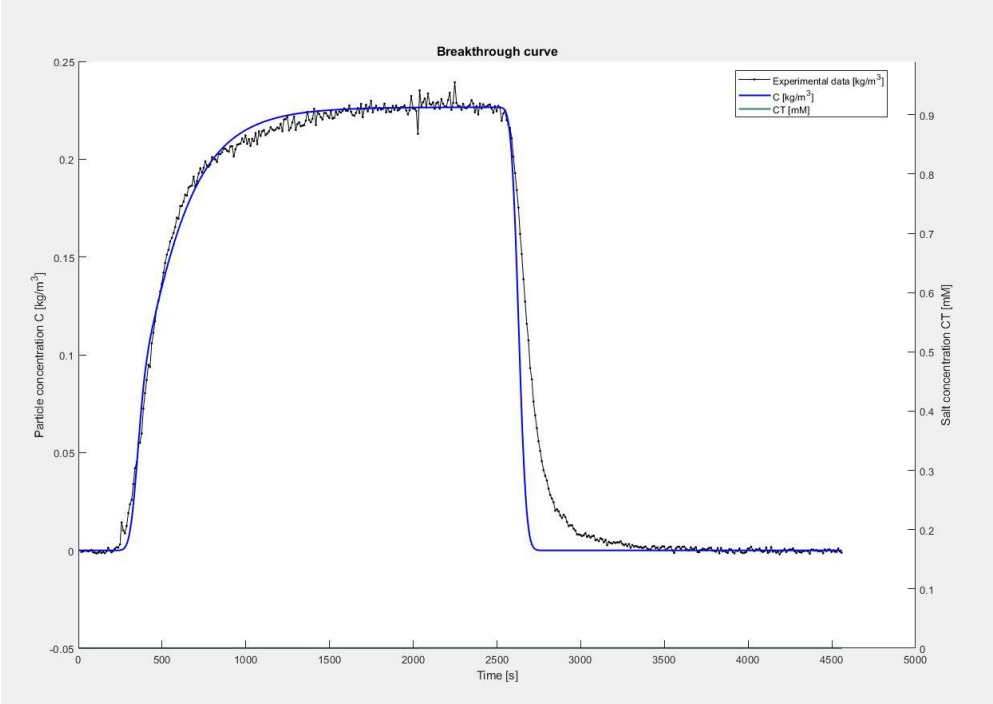

Figure 35: test 'NaCl mod pH 2', transport simulation in MNMs of the formulation with coating prepared in NaCl with modified pH.

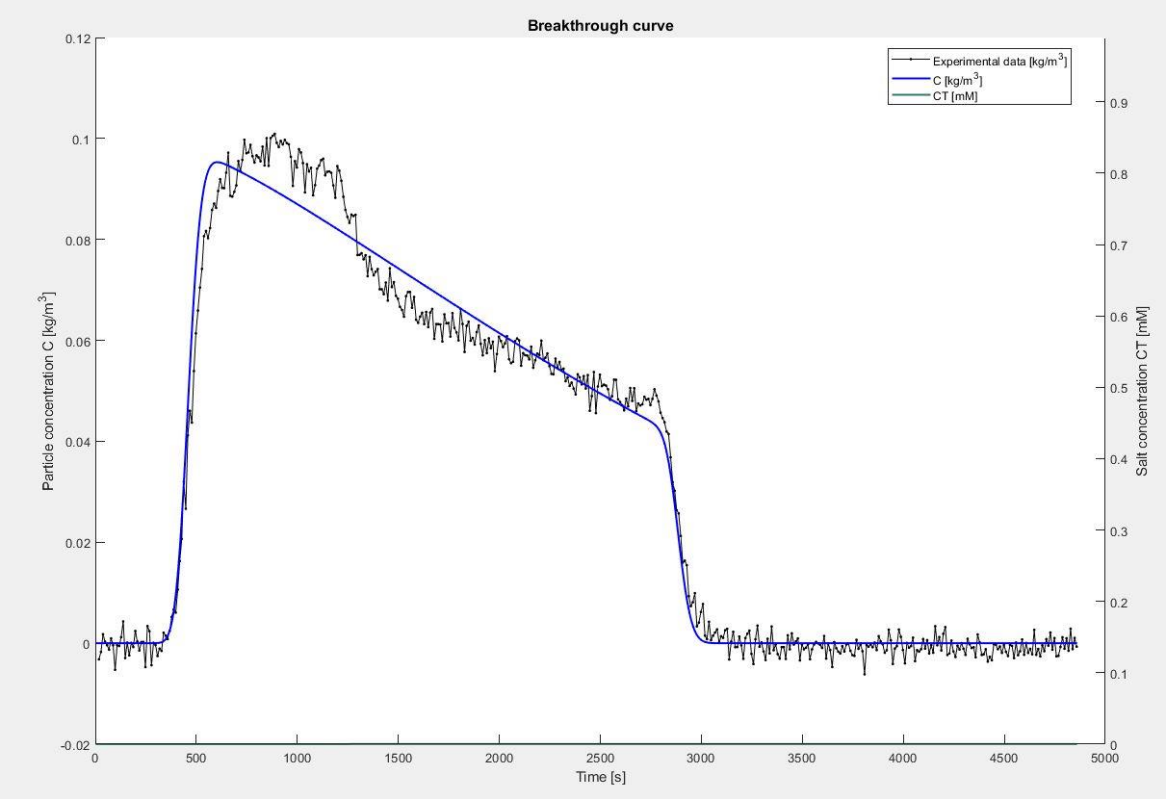

Figure 36: transport simulation in MNMs of clay particles in NaCl.

Unsaturated tracer test water content calculations results

Results from the first tracer test (saturated conditions) for the study of the unsaturated sand column are shown in Table 12. In the same table the calculated values of the remaining water in the column after it is desaturated, θ_d, and of the water injected in the column before injecting the formulation, θ_{in}, and their sum which gives the initial water content in the column before the tracer test in unsaturated conditions is done, are shown.

Table 12: data interpretation of the saturated tracer test for the unsaturated case, estimated parameters in Hydrus 1D and parameters used to calculate the initial water content.

Nano-formulation	Test name	Column length [-]	θ_s-Hydrus [-]	R-2	θ_d [-]	θ_{in} [-]	$\theta_d + \theta_{in}$ [-]
No coating	NaCl 1	0.169	0.31	0.95	0.06	0.09	0.15
	Tap 1	0.165	0.33	0.99	0.04	0.07	0.11
	Tap 2	0.170	0.28	0.97	0.02	0.08	0.10
	NaCl pH mod 1	0.169	0.32	0.98	0.07	0.10	0.17
With coating	NaCl 3	0.169	0.28	0.96	0.04	0.08	0.12
	NaCl 4	0.172	0.32	0.95	0.07	0.05	0.12
	Tap 3	0.168	0.30	0.98	0.05	0.06	0.11
	Tap 4	0.168	0.35	1.00	0.1	0.09	0.19
	NaCl pH mod 2	0.169	0.31	0.94	0.06	0.10	0.16

Nano-herbicide transport test interpretation in unsaturated conditions

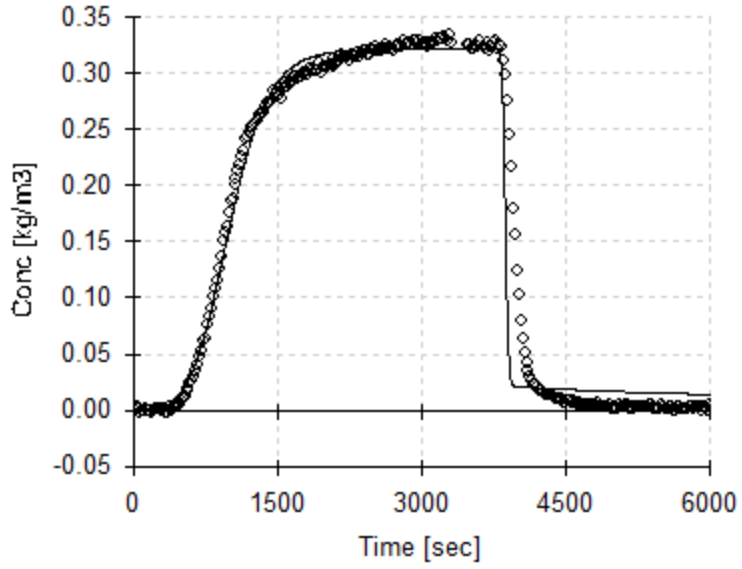

Figure 37: interpretation in Hydrus 1D, test 'tap 3' performed in tap water of the formulation with coating.

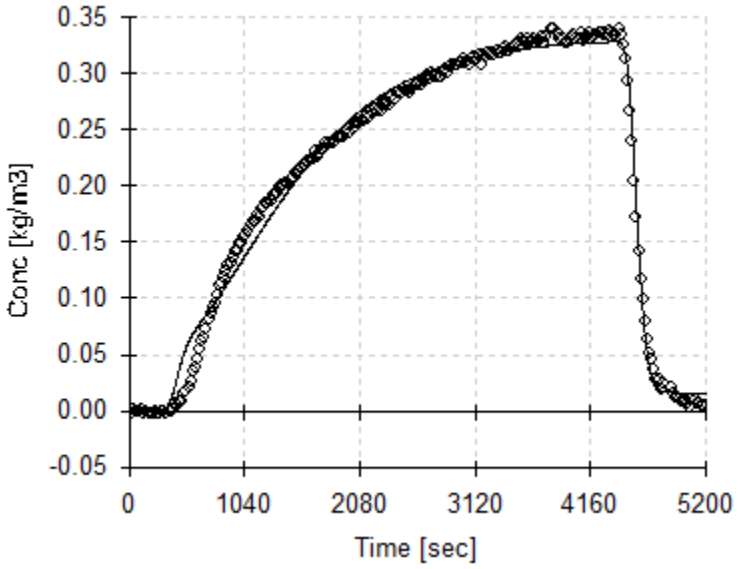

Figure 38: interpretation in Hydrus 1D, test 'tap 4' performed in tap water of the formulation with coating.

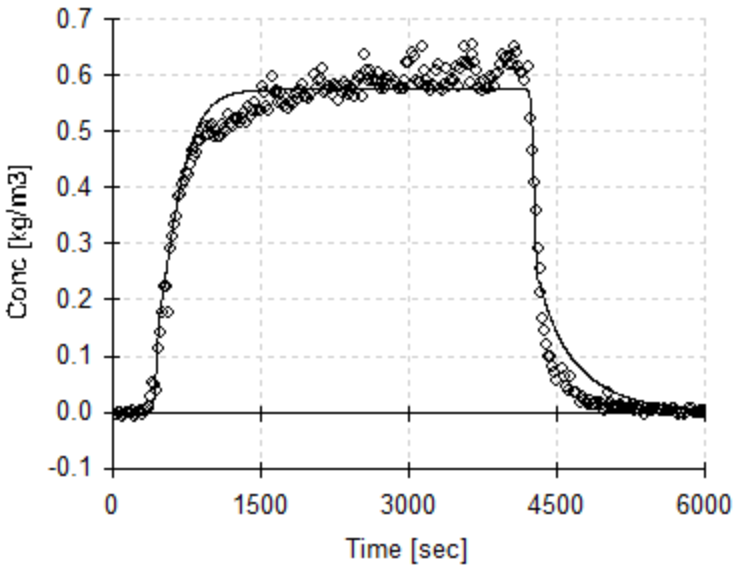

Figure 39: interpretation in Hydrus 1D, test 'Nacl mod pH 2' performed in NaCl at modified pH of the formulation with coating.

Acknowledgement

Firstly, I want to express my gratitude to my supervisor, Prof. Tosco, who has introduced me to the Groundwater Engineering Group and to this fascinating topic. She has always been available, finding the time for suggestions and comments in a tight schedule. I am not sure that saying thank you is enough. Then I want to thank Monica, for her constant availability and support solving issues and for her suggestions when working on this thesis.

When I was welcomed to the Groundwater Engineering Group I had a very good first impression who has never been destroyed: very prepared and friendly people always keen on helping each other. So thanks to everyone for your kindness and for being affable in the everyday life.

My parents, Elisabetta and Franco. I want to immensely thank them for having given me all the instruments to build my life and then having supported and trusted me in everything I wanted to do. I would never be the one I am now without them. Thank you for your constant, unconditional support! Thank to my dad and my mum individually for the inspiring conversations we have had together. My sister, Alice, she deserves special thanks because with her I have the best laughs ever! Thank you for always being there, supporting me and brightening my days.

There are special people who have been part of my life at different time during my master's years, being as supportive as they could, able to wait when I was studying and who have made everything easier in many ways. I am very grateful for having had the pleasure of spending time with them. Other thanks go to my close friends, Alice, Sara, Floriana, Ylenia, Bianca, and Selina. Also when and if geographically far away, they have always been keen on chatting and catching up during the years at university. In these years I am also very grateful for the inspiring personalities I have met, the Green Week organizing team mates in Stockholm, especially Klara and Michael, the Ecopoli students and many others.

Lastly, I want to thank you Politecnico di Torino, and all the people behind it, for offering many chances to feed people with knowledge and life opportunities.

I think I will miss being a student, but I will surely not lose the positive sensation I feel when being curious and when learning new things.